Supporting Information for

Revisiting Biginelli-like Reactions: Solvent Effects, Mechanisms, Biological Applications and Correction of Several Literature Reports

Pedro S. Beck,[a] Arthur G. Leitão,[a] Yasmin B. Santana,[a] José R. Correa,[a] Carime V. S. Rodrigues,[a] Daniel F. S. Machado,[a] Guilherme D. R. Matos,[a] Luciana M. Ramos,[b] Claudia C. Gatto,[a] Sarah C. C. Oliveira,[a] Carlos K. Z. Andrade,[a] and Brenno A. D. Neto,*[a]

[a] University of Brasilia, Chemistry Institute, Laboratory of Medicinal and Technological Chemistry. Campus Universitário Darcy Ribeiro, Brasília, DF, 70910-900, Brazil. E-mail: brenno.ipi@gmail.com.

[b] Universidade Estadual de Goiás (UEG), Anápolis, Goiás, 75001-970, Brazil.

[c] University of Brasilia, Institute of Biology, Laboratory of Allelopathy, Campus Universitário Darcy Ribeiro, Brasília, DF, 70910-900, Brazil.

Table of Content

List of Schemes

List of Tables

List of Figures

Schemes

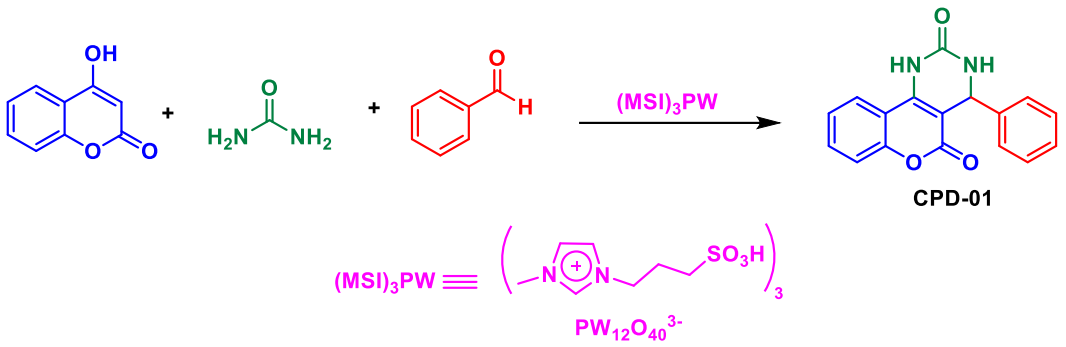

Scheme S1. Synthesis reaction for the claimed structure of **CPD-01** utilizing the superacid imidazolium-based ionic liquid MSI_3PW.

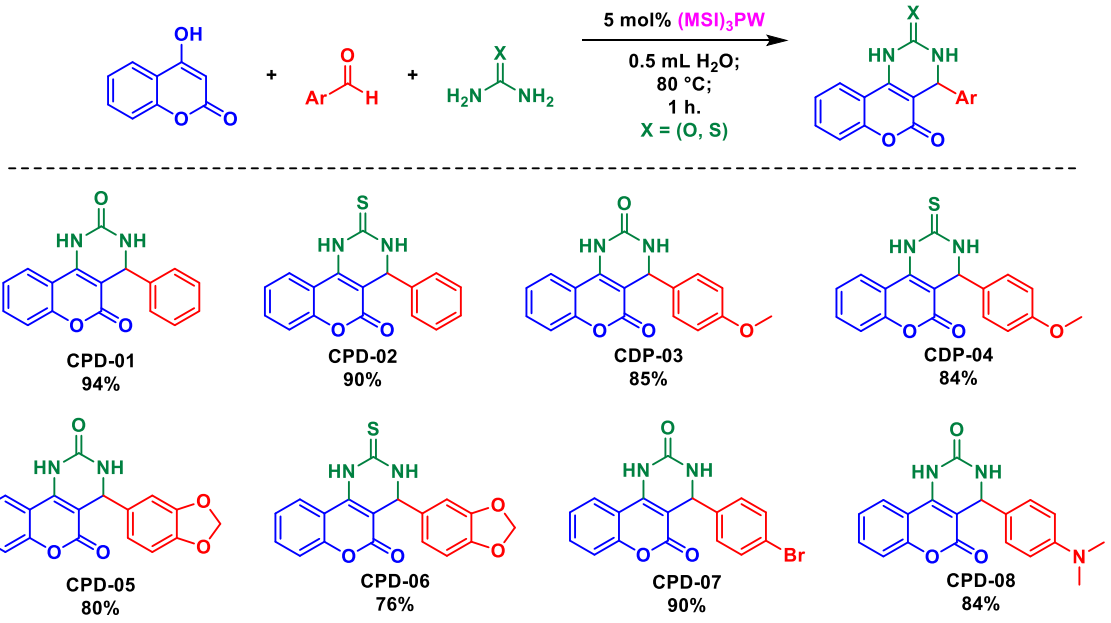

Scheme S2. Synthesis of the claimed **CPD** adducts and their respective yields based on their theoretical masses.

Tables

Table S1. Kamlet-Taft descriptors, yields for the claimed **CPD** as a function of solvent variation and reagents' proportions, and E-factors.

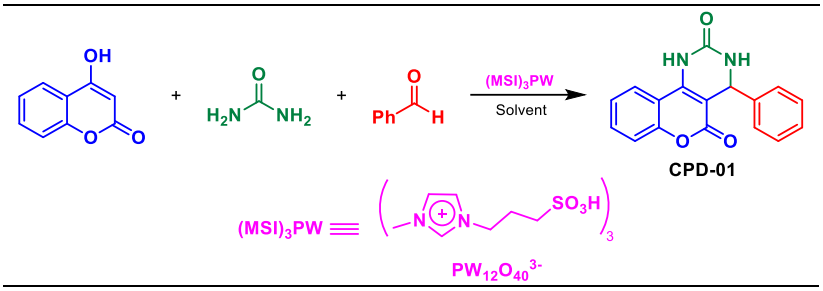

		Isolated yields (%)				
		Reagents' proportion (mmol) Coumarin : Aldehyde : Urea				
Solvent	**Kamlet-Taft descriptors**	**1:1:1**	**2:1:1**	**1:2:1**	**1:1:2**	**E factor†**
AcOEt	α 0.00 β 0.45 π* 0.55	74%	67%	72%	62%	47
MeCN	α 0.19 β 0.31 π* 0.75	63%	85%	65%	53%	41
Water	α 1.17 β 0.47 π* 1.09	94%	94%	90%	71%	36
$[C_4C_1Im][BF_4]$	α 0.63 β 0.38 π* 1.04	69%	93%	83%	77%	38
$[C_4C_1Im][NTf_2]$	α 0.62 β 0.23 π* 0.90	80%	90%	88%	59%	39
$[C_4C_1Im][PF_6]$	α 0.63 β 0.19 π* 1.02	71%	94%	75%	64%	37
CH_2Cl_2	α 0.04 β -0.01 π* 0.79	74%	79%	80%	75%	44
EtOH	α 0.83 β 0.75 π* 0.51	77%	90%	75%	58%	39
Hexane	α -0.08 β 0.00 π* 0.00	53%	63%	59%	44%	55
MeOH	α 0.93 β 0.66 π* 0.58	65%	92%	82%	52%	38
PhMe	α 0.00 β 0.11 π* 0.54	55%	72%	75%	50%	47

† Calculated for the best yield of each solvent.

Table S2. Melting point (mp) evaluation for the claimed **CPD-01** structure reported in the literature.

Year of publication	mp (°C)	Reference
2003	-	1
2006	162	2
2008	162-163	3
2014	210-212	4
2015	265-267	5
2016	162-163	6
2016	160-162	7
2017	160-162	8
2018	160-162	9
2018	160-162	10
2018	206	11
2018	160-162	12
2018	238-240	13
2019	165-167	14
2019	160-162	15
2020	163-165	16
2020	211-213	17
2020	160-162	18
2022	162-163	19
2022	160-162	20
2023	214-216	21
2023	210-212	22

Table S3. A comparative assessment of experimental versus theoretical elemental analysis (CHN) data for alleged **CPDs** structures. Specifically, for claimed **CPD-01**, the data reveals a composition wherein approximately two molecules of **DC-01** correlate with nearly one molecule of urea/thiourea.

	Experimental Data			Theorical Data		
Structure	**Carbon (%)**	**Hydrogen (%)**	**Nitrogen (%)**	**Carbon (%)**	**Hydrogen (%)**	**Nitrogen (%)**
CPD-01	64.62	3.92	2.90	69.86	4.14	9.58
CPD-02	63.59	3.47	0.48	66.22	3.92	9.08
CPD-03	68.65	3.95	0.13	67.08	4.38	8.69
CPD-04	53.33	2.85	0.06	63.89	4.17	8.28
CPD-05	67.29	3.36	0.07	64.29	3.6	8.33
CPD-06	64.04	3.25	0.01	61.36	3.43	7.95
CPD-07	56.01	2.82	1.32	55.01	2.99	7.55
CPD-08	70.53	4.49	2.98	68.05	5.11	12.53

Table S4. Indicative of whether these articles provide descriptions and/or FTIR spectra for the claimed **CPD-01**.

Year of publication	Experimental description	Available Spectrum	Reference
2003	-	-	1
2006	Yes	No	2
2008	Yes	No	3
2014	Yes	No	4
2015	Yes	No	5
2016	Yes	No	6
2016	Yes	No	7
2017	Yes	No	8
2018	Yes	No	9
2018	No	No	10
2018	Yes	No	11
2018	No	No	12
2018	Yes	Yes	13
2019	No	No	14
2019	Yes	No	15
2020	Yes	No	16
2020	No	Yes	17
2020	Yes	No	18
2022	Yes	No	19
2022	Yes	Yes	20
2023	Yes	Yes	21
2023	No	No	22

Table S5. Indicative of whether these articles provide descriptions and/or mass spectra for claimed **CPD-01**.

Year of publication	Experimental Description	Ionization Source / (*m/z* detected)	Available Spectrum	Reference
2003	-		-	1
2006	No		No	2
2008	Yes	Not available / (292.0)	No	3
2014	No		No	4
2015	No		No	5
2016	No		No	6
2016	Yes	ESI-(+) / (292.3)	No	7
2017	No		No	8
2018	No		No	9
2018	Yes	ESI-(+) / (292.3)	Yes	10
2018	No		No	11
2018	Yes	ESI-(+) / (292.3)	Yes	12
2018	Yes	Not available / (292)	No	13
2019	No		No	14
2019	Yes	ESI-(+) / (292.3)	Yes	15
2020	Yes	ESI-(+) / (293.3)	No	16
2020	No		No	17
2020	No		No	18
2022	Yes	Not available / (292.0)	No	19
2022	No		No	20
2023	No		No	21
2023	No	No	No	22

Table S6. Indicative of whether these articles provide descriptions and/or ^{1}H and ^{13}C NMR spectra for claimed **CPD-01**.

Year	^{1}H NMR		^{13}C NMR		Reference
	Experimental Description	Available spectrum	Experimental Description	Available spectrum	
2003	-	-	-	-	1
2006	Yes	No	No	No	2
2008	Yes	No	No	No	3
2014	Yes	No	Yes	No	4
2015	Yes	No	Yes	No	5
2016	Yes	No	No	No	6
2016	Yes	Yes*	Yes	Yes	7
2017	Yes	No	No	No	8
2018	Yes	No	Yes	No	9
2018	Yes	Yes*	Yes	Yes*	10
2018	Yes	No	Yes	No	11
2018	Yes	Yes*	Yes	Yes*	12
2018	Yes	Yes	Yes	No	13
2019	Yes	Yes	No	No	14
2019	Yes	Yes*	Yes	Yes*	15
2020	Yes	No	Yes	No	16
2020	No	No	No	No	17
2020	Yes	No	Yes	No	18
2022	Yes	No	No	No	19
2022	No	No	No	No	20
2023	Yes	Yes	No	No	21
2023**	No	No	No	No	22

* Indicate the articles that likely have duplicate spectra among themselves. ** Available spectra for similar structures, but not for **CPD-01**.

Table S7. Indicative of whether these articles show descriptions for elemental analysis and accuracy with respect to the expected values for the claimed **CPD-01** structure.

Year of publication	Experimental Description	Accuracy	Calculate (%)	Found (%)	Reference
2003	-	-	-	-	1
2006	Yes	Yes	C 69.88 H 4.10 N 9.58	C 69.80 H 4.01 N 9.49	2
2008	Yes	Yes	C 69.86 H 4.10 N 9.58	C 69.85 H 4.14 N 9.56	3
2014	No	-	-	-	4
2015	Yes	Yes	C 69.86 H 4.14 N 9.58	C 69.67 H 4.11 N 9.61	5
2016	Yes	No*(a)	C 69.86 H 4.14 N 9.58	C 69.64 H 3.96 N 9.69	6
2016	No	-	-	-	7
2017	No	-	-	-	8
2017	No	-	-	-	9
2018	Yes	Yes	C 69.86 H 4.14 N 9.58	C 70.02 H 4.18 N 9.69	10
2018	No	-	-	-	11
2018	Yes	Yes	C 69.86 H 4.14 N 9.58	C 70.02 H 4.18 N 9.69	12
2018	Yes	Yes	C 69.86 H 4.14 N 9.58	C 70.00 H 4.27 N 9.60	13
2019	No	-	-	-	14
2019	Yes	Yes	C 69.86 H 4.14 N 9.58	C 70.02 H 4.18 N 9.69	15
2020	Yes	Yes	Not available	C 69.86 H 4.14 N 9.58	16
2020	No	-	-	-	17
2020	Yes	Yes	C 69.86 H 4.14 N 9.58	C 69.92 H 4.22 N 9.70	18
2022	Yes	No*(b)	C 69.86 H 4.10 N 9.58	C 69.85 H 4.14 N 5.30	19
2022	No	-	-	-	20
2023	No	-	-	-	21
2023	No	-	-	-	22

* = Chemical formula calculated based on experimental CHN: (a) $C_{17}H_{11}N_2O_3$; (b) $C_{31}H_{22}N_2O_7$. The results of elemental analyses in red highlight that the values have been triplicated in different publications. The value highlighted in blue indicates that the obtained value is exactly equal to the theoretical value.

Table S8. Exploring reaction condition variations in the attempt to synthesize **PCC-01**.[a]

Entry	Solvent	Temperature (°C)	Time	Catalyst	Product	Yield
1	Ethanol	50	30 min	HCl	**DC-01**	51%
2	Ethanol	60	30 min	HCl	**DC-01**	53%
3	Ethanol	70	30 min	HCl	**DC-01**	52%
4	Ethanol	80	30 min	HCl	**DC-01**	44%
5	Ethanol	90	30 min	HCl	**DC-01**	48%
6	Ethanol	100	30 min	HCl	**DC-01**	44%
7	Ethanol	60	2 h	HCl	**DC-01**	47%
8	Ethanol	60	3 h	HCl	**DC-01**	44%
9	Ethanol	60	4 h	HCl	**DC-01**	44%
10	Ethanol	60	5 h	HCl	**DC-01**	45%
11	Ethanol	60	6 h	HCl	**DC-01**	48%
12	Ethanol	70	6 h	HCl	**DC-01**	43%
13	Ethanol	80	6 h	HCl	**DC-01**	42%
14	Ethanol	90	6 h	HCl	**DC-01**	43%
15	Ethanol	100	6 h	HCl	**DC-01**	47%
16	Ethanol	60	24 h	HCl	**DC-01**	44%
17	Ethanol	100	24 h	HCl	**DC-01**	38%
18	Ethanol	60	48 h	HCl	**DC-01**	48%
19	Ethanol	100	48 h	HCl	**DC-01**	38%
20	Ethanol	60	30 min	$(MSI)_3PW$	**DC-01**	73%
21	Ethanol	60	24 h	$(MSI)_3PW$	**DC-01**	81%
22	Ethanol	100	30 min	$(MSI)_3PW$	**DC-01**	55%
23	Ethanol	100	24 h	$(MSI)_3PW$	**DC-01**	88%
24	Ethanol	60	30 min	KOtBu	**DC-01**	65%
25	Ethanol	60	24 h	KOtBu	**DC-01**	80%
26	*t*-Butanol	60	30 min	KOtBu	**DC-01**	66%
27	*t*-Butanol	60	24 h	KOtBu	**DC-01**	65%
28	Solventless	60	15 min	MWI[b]	**DC-01**	40%

[a] No condition allowed the formation of **ACP-01**. [b] Microwave irradiation.

Table S9. Kamlet-Taft parameters used for solvent effect analysis.

Solvent	α	β	π*
1,4-Dioxane	0.00	0.37	0.55
Acetone	0.08	0.43	0.71
AcOEt	0.00	0.45	0.55
$BMI.BF_4$	0.63	0.38	1.04
$BMI.NTf_2$	0.62	0.23	0.90
$BMI.PF_6$	0.63	0.38	1.04
CF_3CH_2OH	1.51	0.00	0.73
$CHCl_2$	0.04	-0.01	0.79
$CHCl_3$	0.20	0.10	0.58
Cyclohexane	0.00	0.00	0.00
EtOH	0.83	0.75	0.51
H_2O	1.17	0.47	1.09
Hexane	-0.08	0.00	0.00
Limonene	0.00	0.00	0.16
MeCN	0.19	0.31	0.75
MeOH	0.93	0.66	0.58
n-OcOH	0.77	0.81	0.4
p-Cymene	0.00	0.13	0.39
t-BuOH	0.68	0.93	0.41
THF	0.00	0.55	0.58
Toluene	0.00	0.11	0.54
Triethylamine	0.00	0.71	0.14

Figures

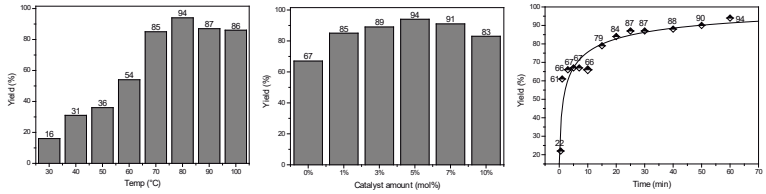

Figure S1. Conditions optimization for the attempts to synthesize **CPD-01**. (Left) Temperature optimization. (Center) Catalyst amount optimization. (Right) Time optimization.

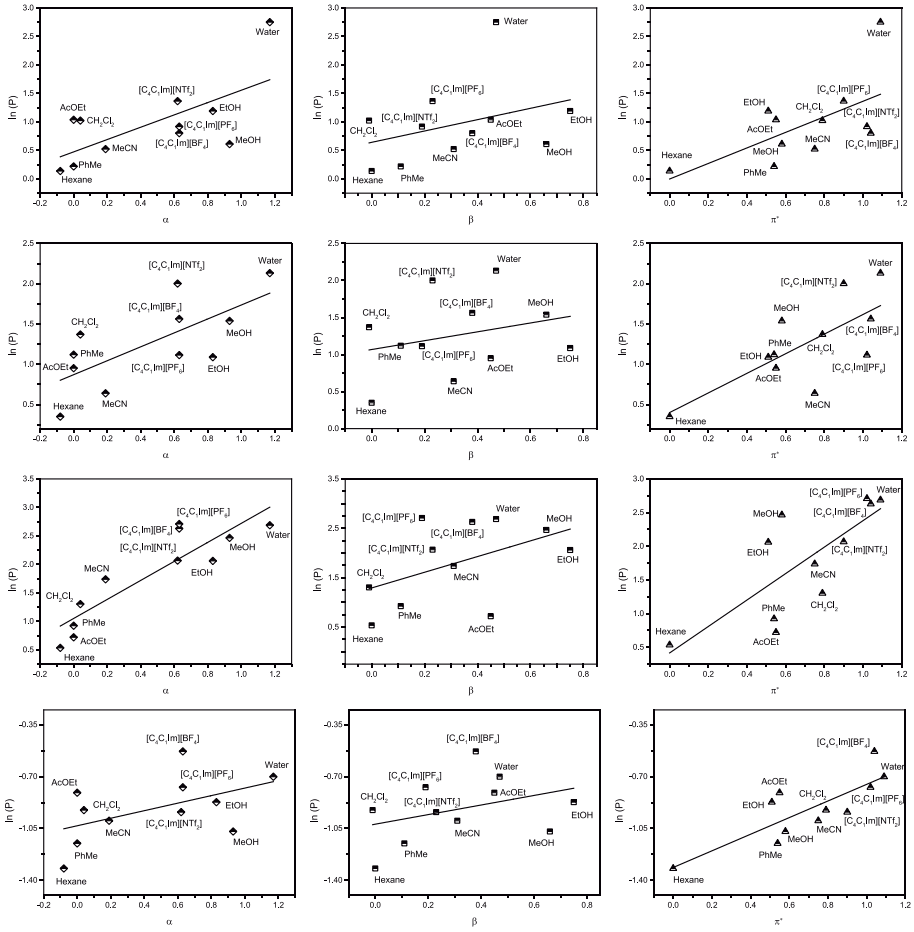

Figure S2. Correlations of reaction productivity (expressed as ln(P)) as a function of Kamlet-Taft parameters (α, β and π*). All data refer to isolated yields of the model reaction (benzaldehyde, 4-hydroxycoumarin, and urea mixtures, 5 mol% of the catalyst at 80 °C for 60 min). Reactions proportion (mmol) from top to bottom: (i) Equimolar conditions i.e. 1.00 (benzaldehyde) : 1.00 (coumarin) : 1.00 (urea). (ii) Aldehyde excess i.e. 2.00 (benzaldehyde) : 1.00 (coumarin) : 1.00 (urea). (iii) Coumarin excess i.e. 1.00 (benzaldehyde) : 2.00 (coumarin) : 1.00 (urea). (iv) Urea excess i.e. 1.00 (benzaldehyde) : 1.00 (coumarin) : 2.00 (urea).

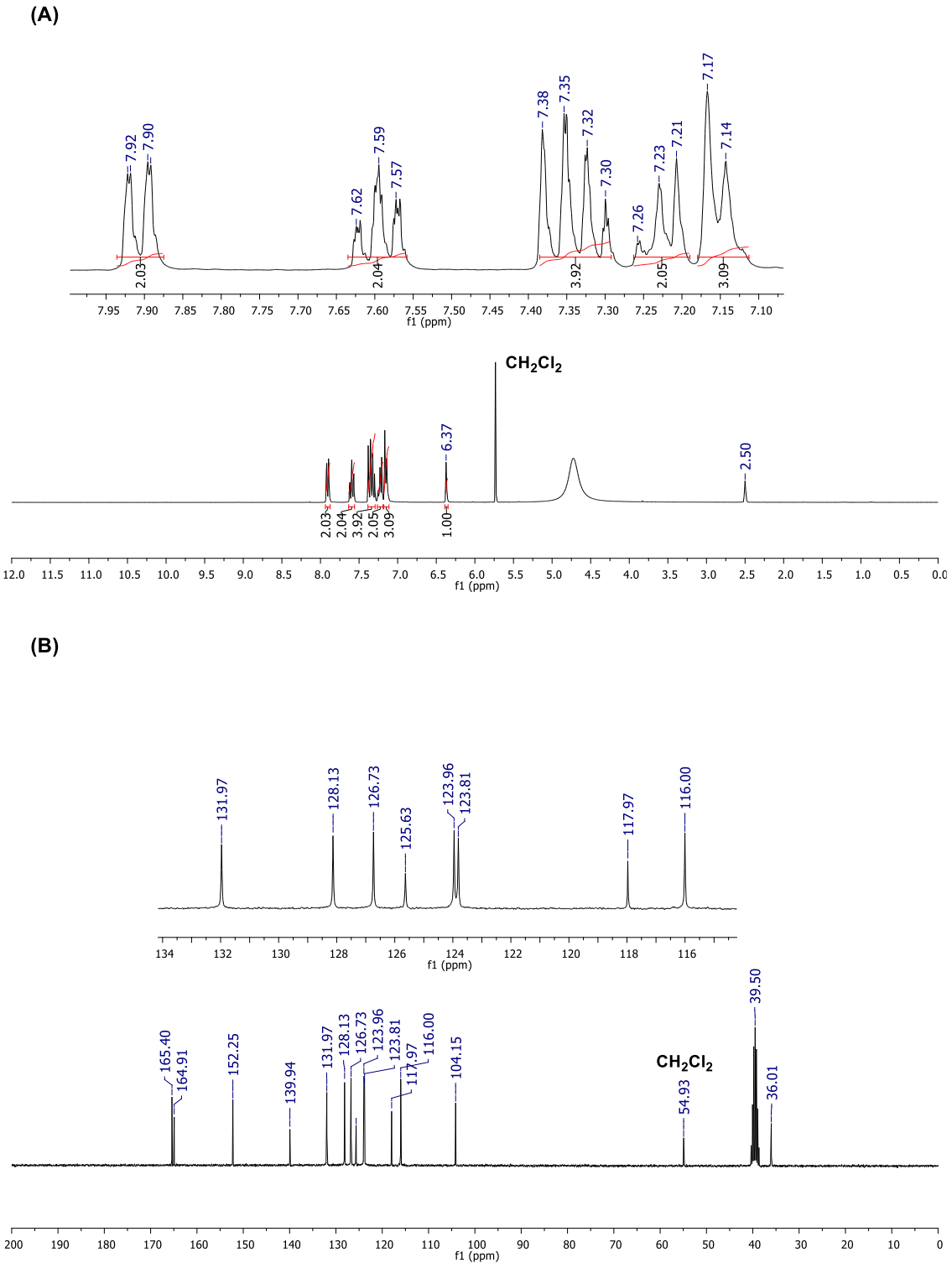

Figure S3. (A) ^{1}H NRM (DMSO-d_6, 300 MHz) for claimed **CPD-01** adduct. (B) ^{13}C{^{1}H} NRM (DMSO-d_6, 75 MHz) for claimed **CPD-01** adduct. These two spectra are contaminated with urea. Note the number of hydrogens and carbons do not fit the claimed **CPD-01** structure.

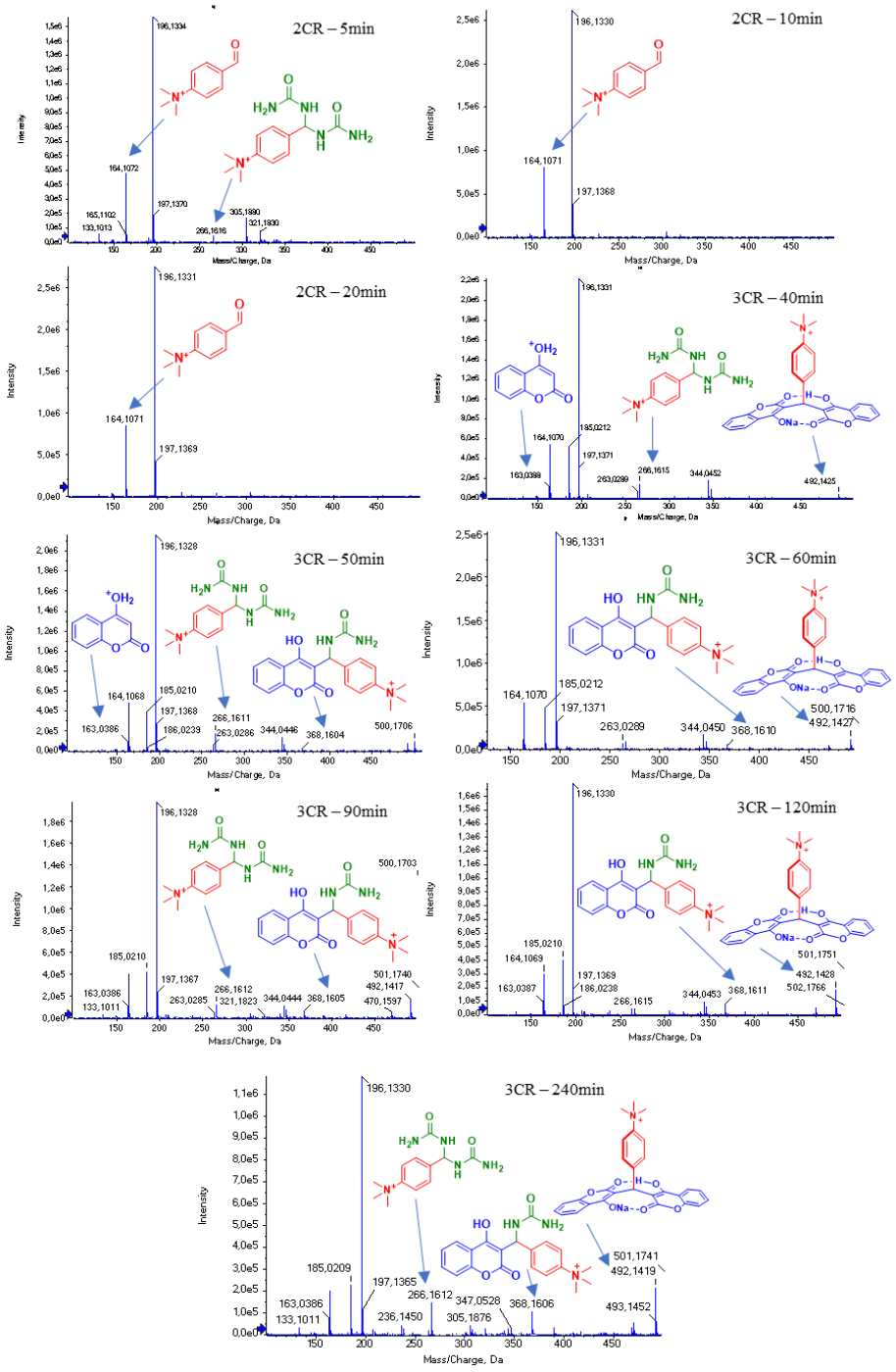

Figure S4. Reaction monitoring by HRMS using *p*-cymene as the solvent and at 80 °C.

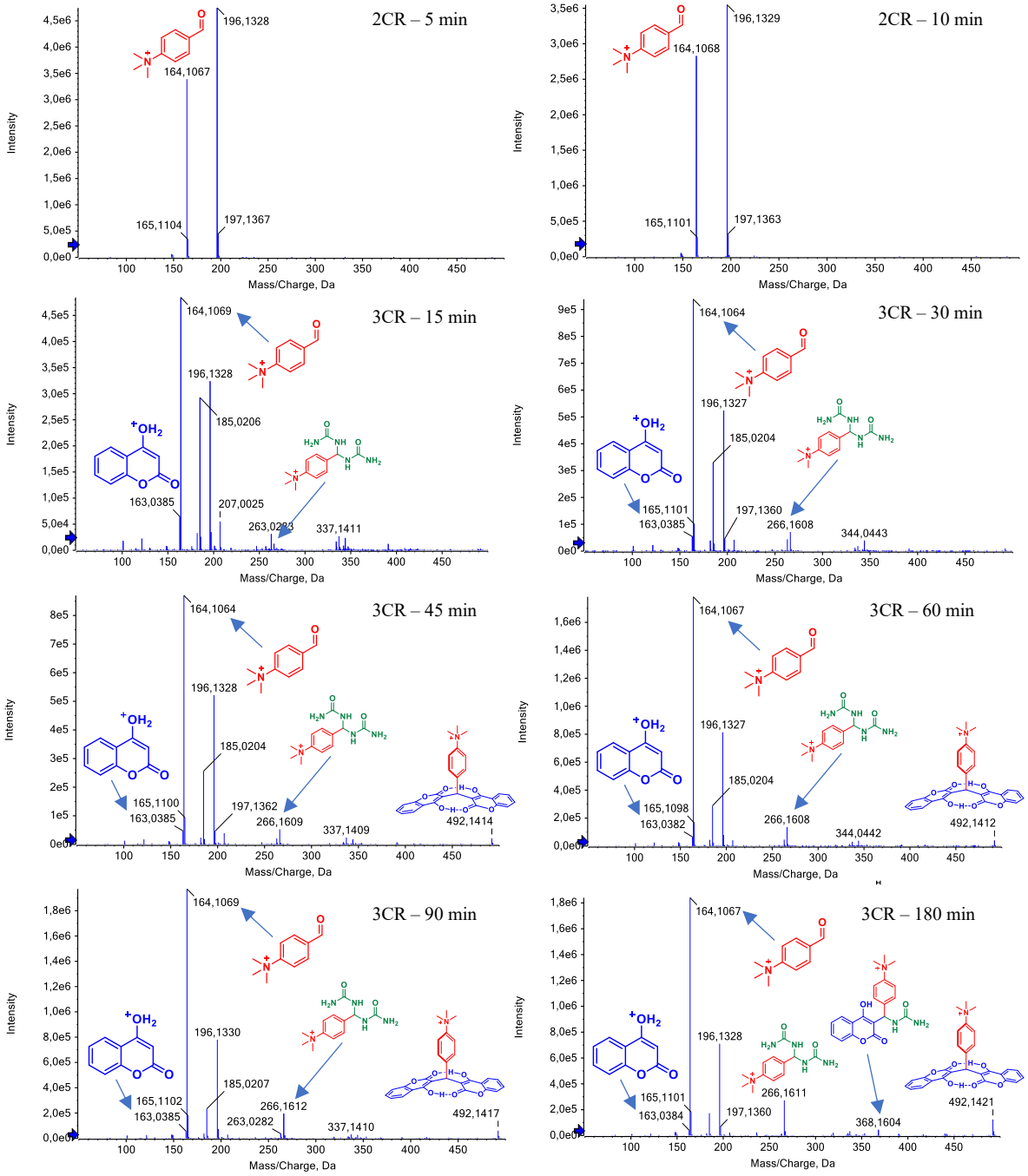

Figure S5. Reaction monitoring by HRMS using limonene as the solvent and at 80 °C.

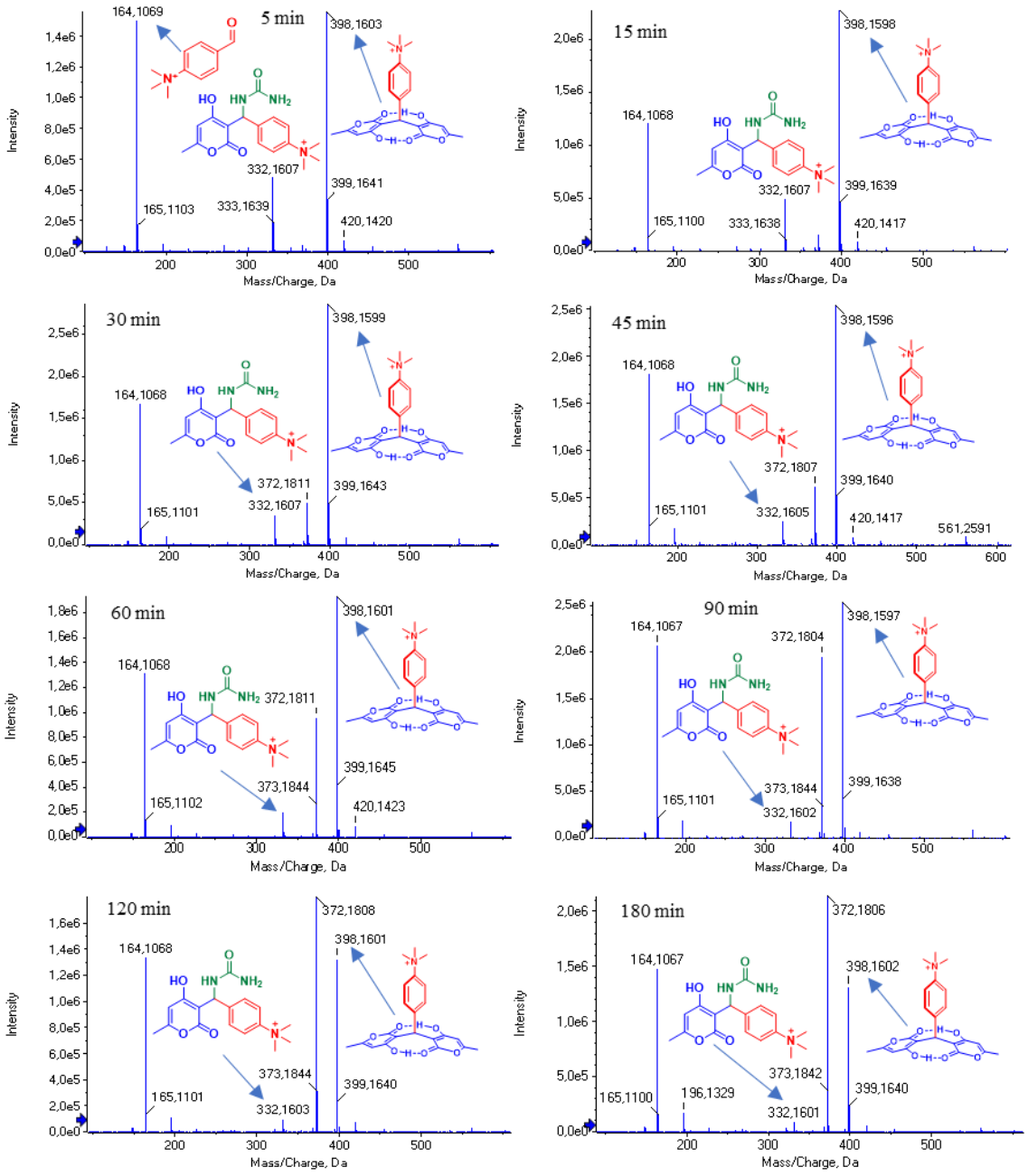

Figure S6. Reaction monitoring by HRMS using water as the solvent and at 80 °C.

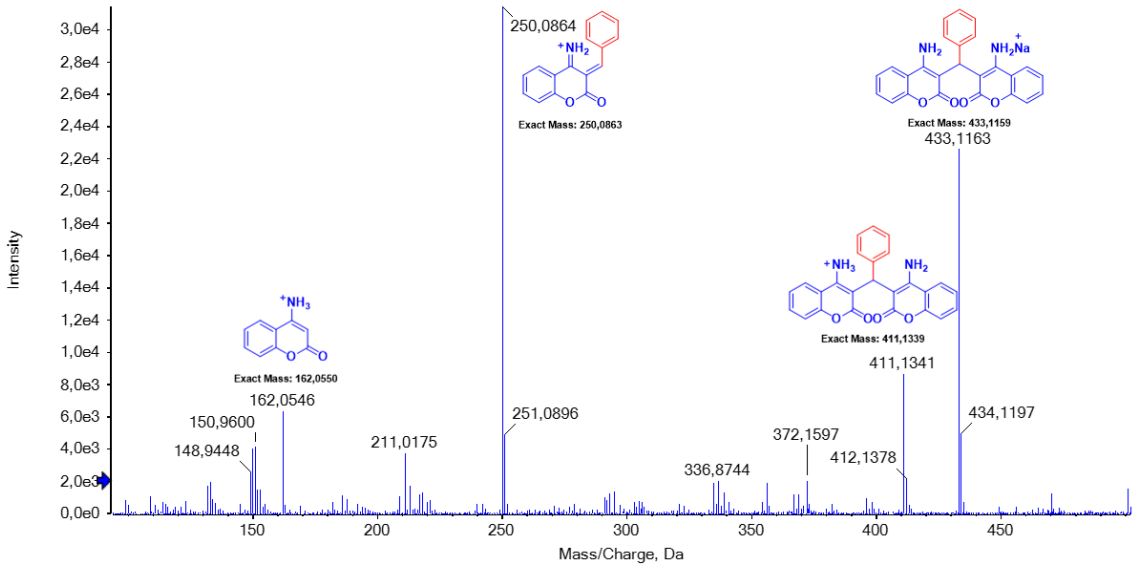

Figure S7. Reaction monitoring by HRMS using water as the solvent and at 100 °C. 4-Aminocoumarin was used instead of 4-hydroxycoumarin.

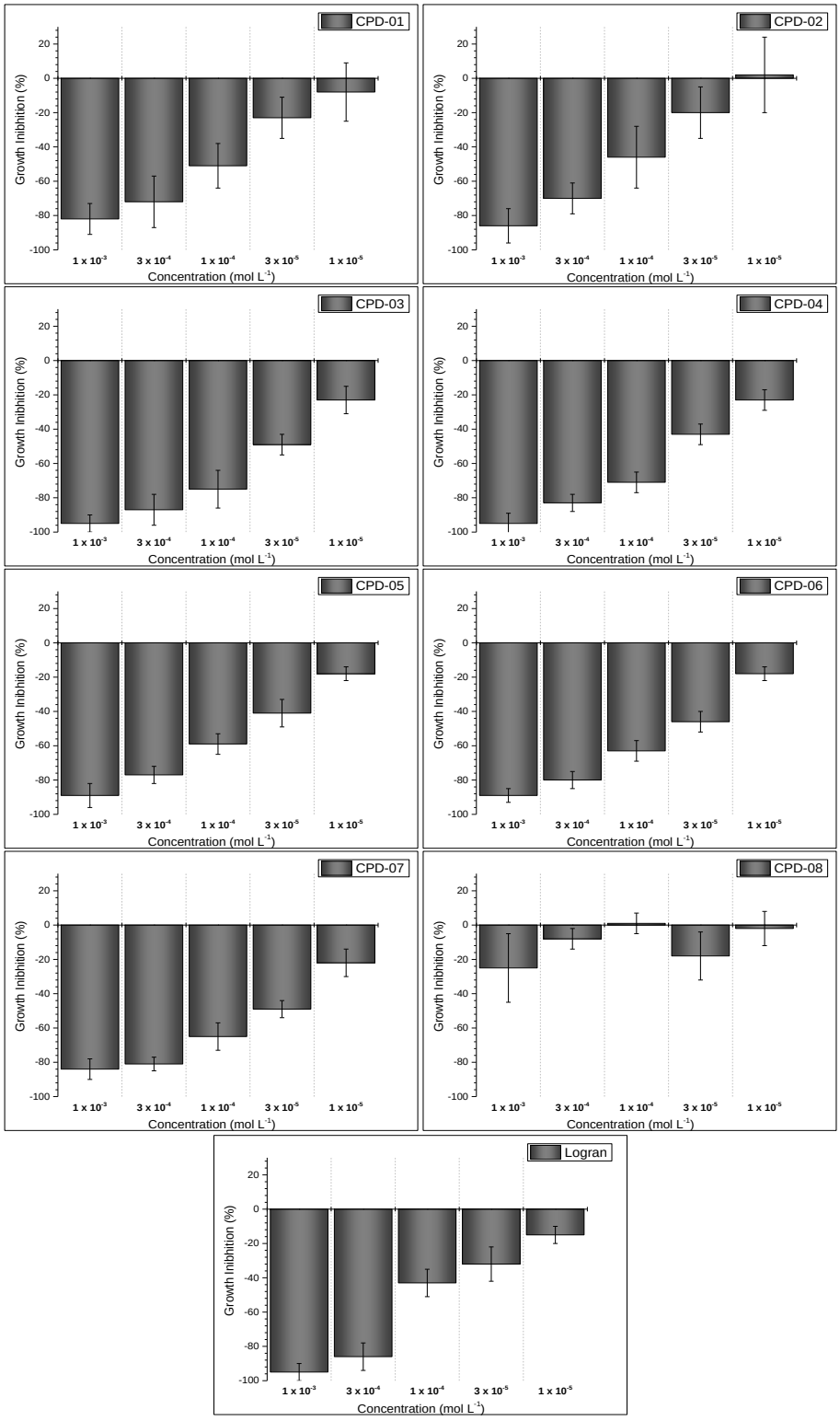

Figure S8. Wheat coleoptile bioassay testing the synthesized **DC** derivatives contaminated with urea or thiourea (proportion of ≈ 2 **DC** : 1 urea/thiourea). Logran is the positive control. **CDPs 01**, **03**, **05**, **07** and **08** are indeed and respectively **DCs 01**, **02**, **03**, **04** and **05** contaminated with urea. **CPDs 02, 04** and **06** are respectively **DCs 01**, **02**, **03**, contaminated with thiourea.

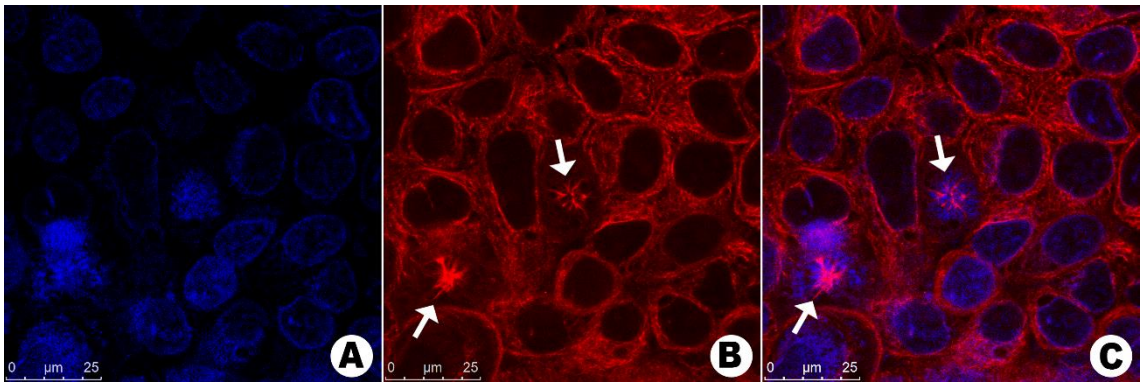

Figure S9. Cellular division (mitosis) inhibition by **DC-03** contaminated with urea (proportion of ≈ 2 **DC** : 1 urea/thiourea). (A) Nuclei stained with the commercially available DAPI (blue emitter). (B) Anti-α-Tubulin monoclonal antibody (commercially available red emitter). (C) Merged images from (A)-(B). Remarkably, despite the presence of those contaminant, **DC-03** induced monoastral spindles in mitotic cells.

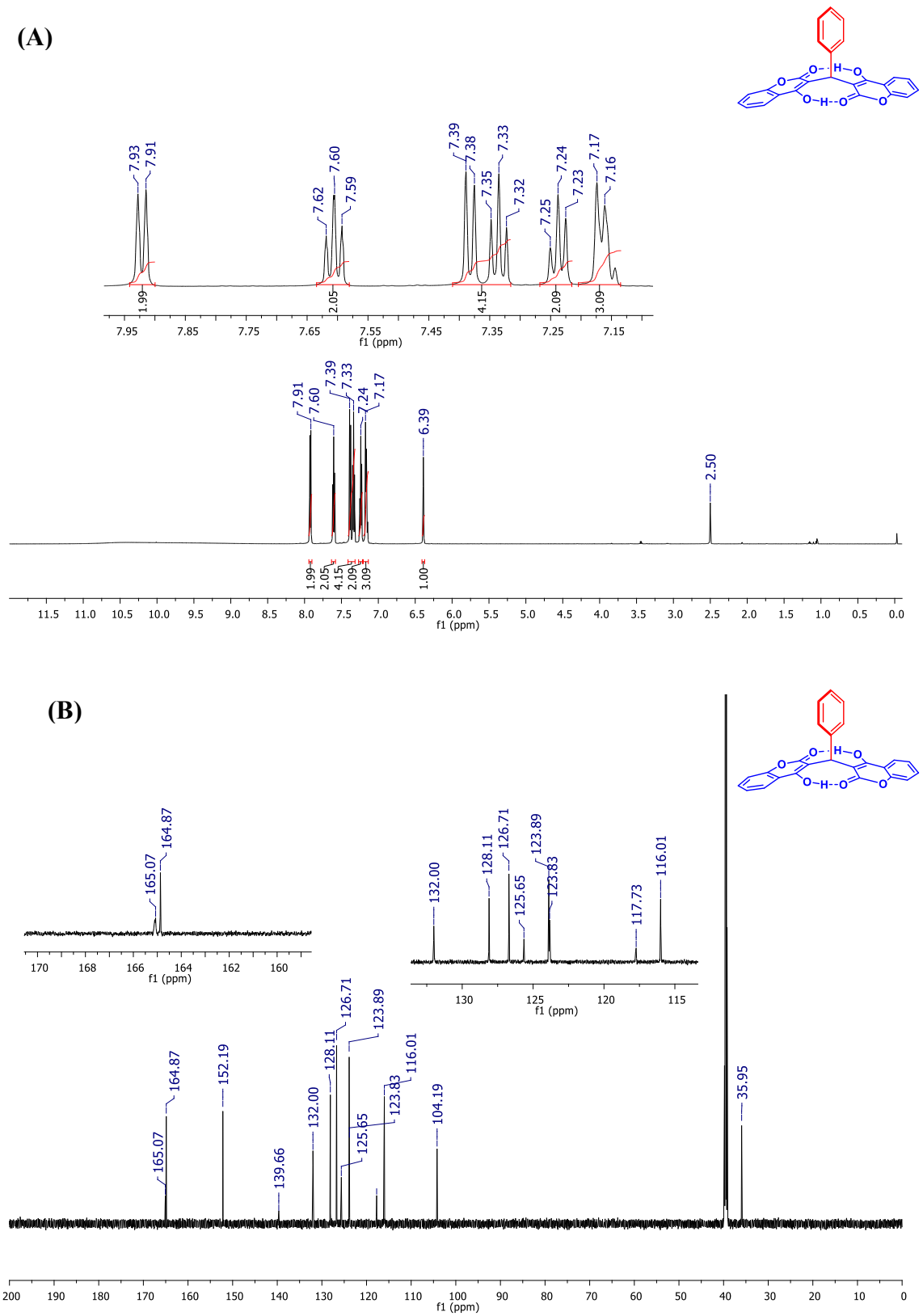

Figure S10. (A) ^{1}H NMR spectrum (600 MHz, DMSO-d_6) of **DC-01.** (B)^{13}C{^{1}H} NMR spectrum (150 MHz, DMSO-d_6) of **DC-01**.

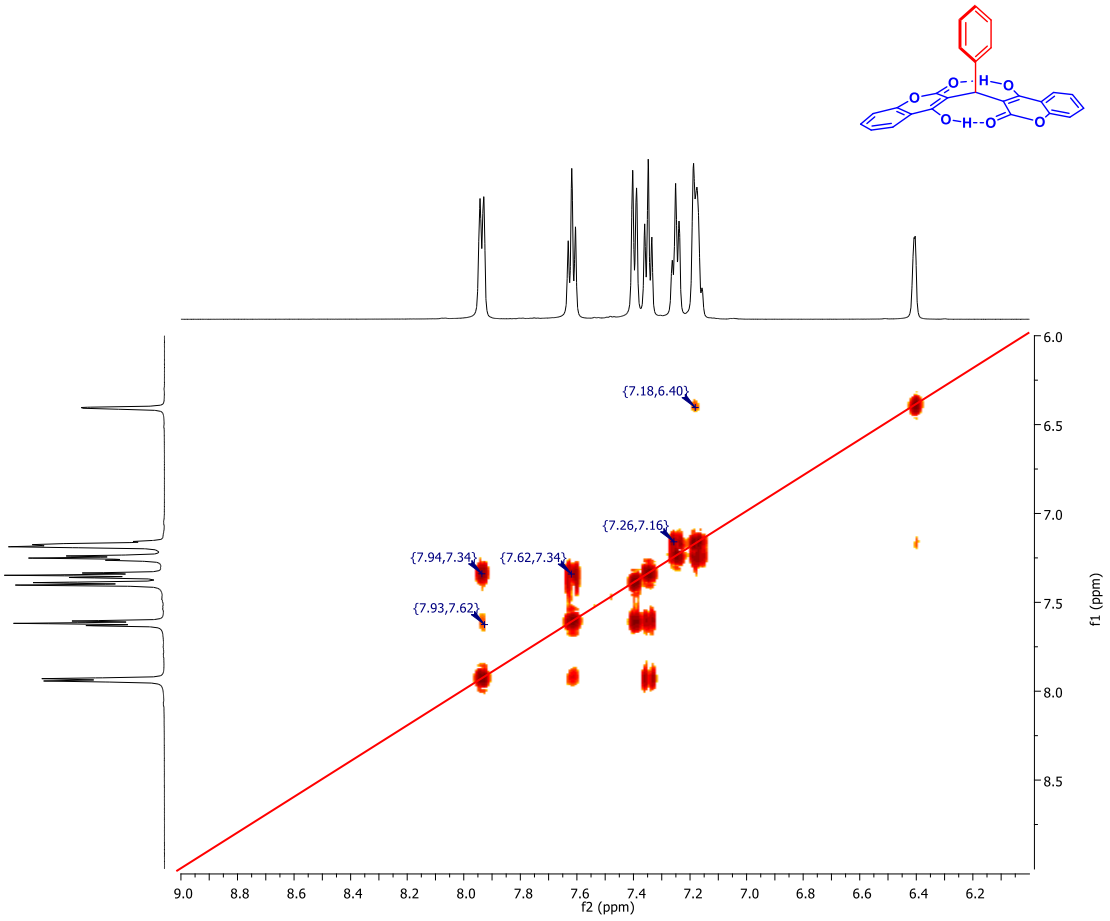

Figure S11. 2D COSY NMR (600 MHz, DMSO-d_6) for **DC-01**.

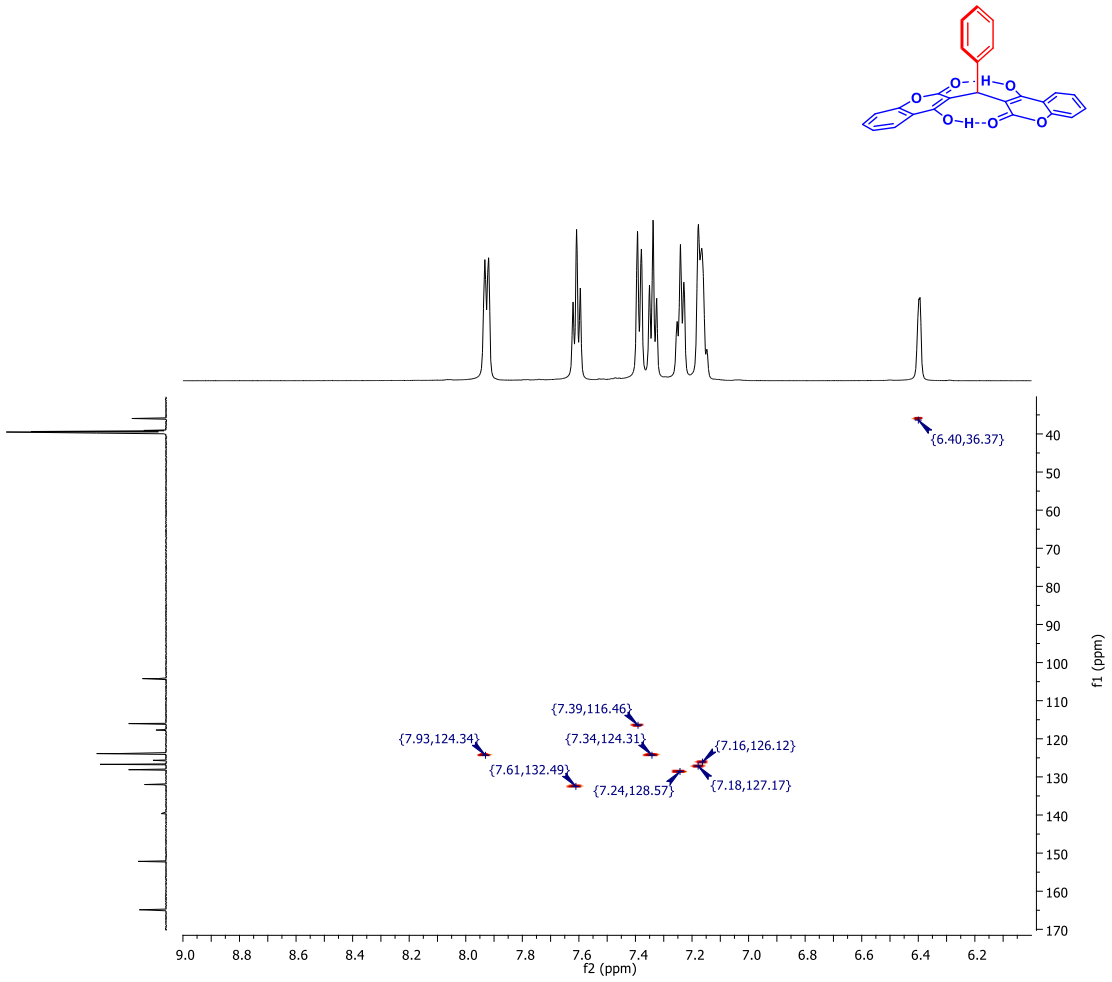

Figure S12. 2D HSQC NMR (600 MHz and 150 MHz, DMSO-d_6) for **DC-01**.

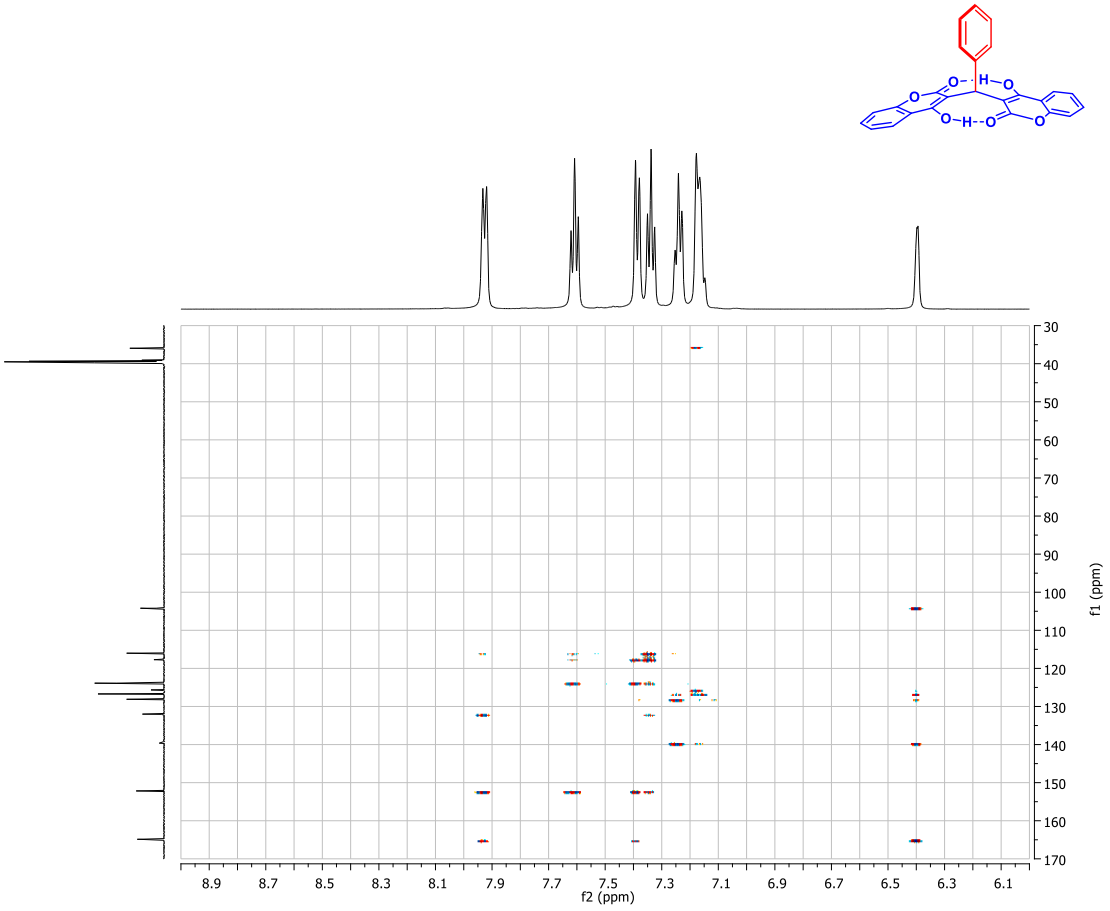

Figure S13. 2D HMBC (600 MHz and 150 MHz, DMSO-d_6) for **DC-01**.

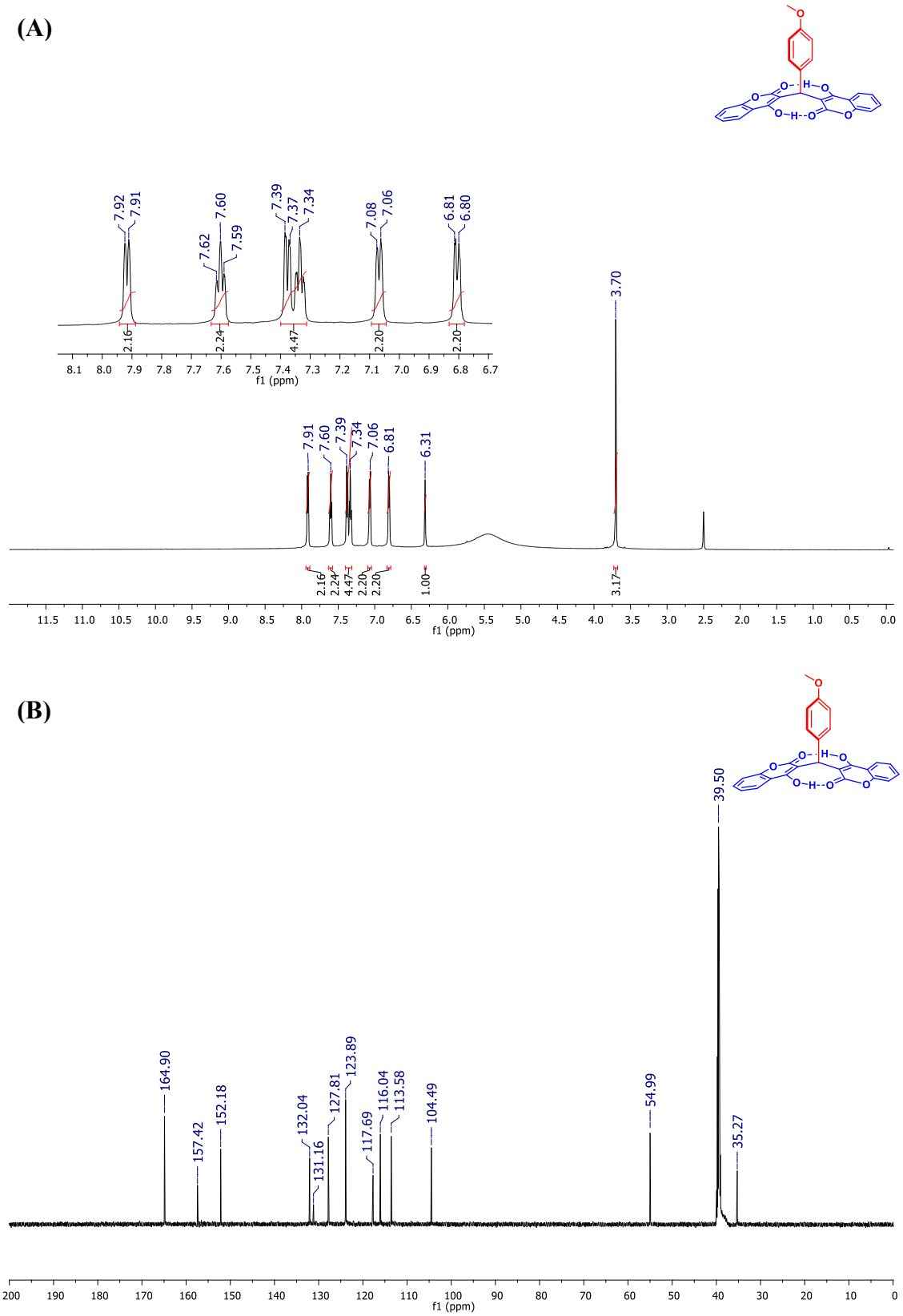

Figure S14. (A) ^{1}H NMR spectrum (600 MHz, DMSO-d_6) of **DC-02.** (B)^{13}C{^{1}H} NMR spectrum (150 MHz, DMSO-d_6) of **DC-02**.

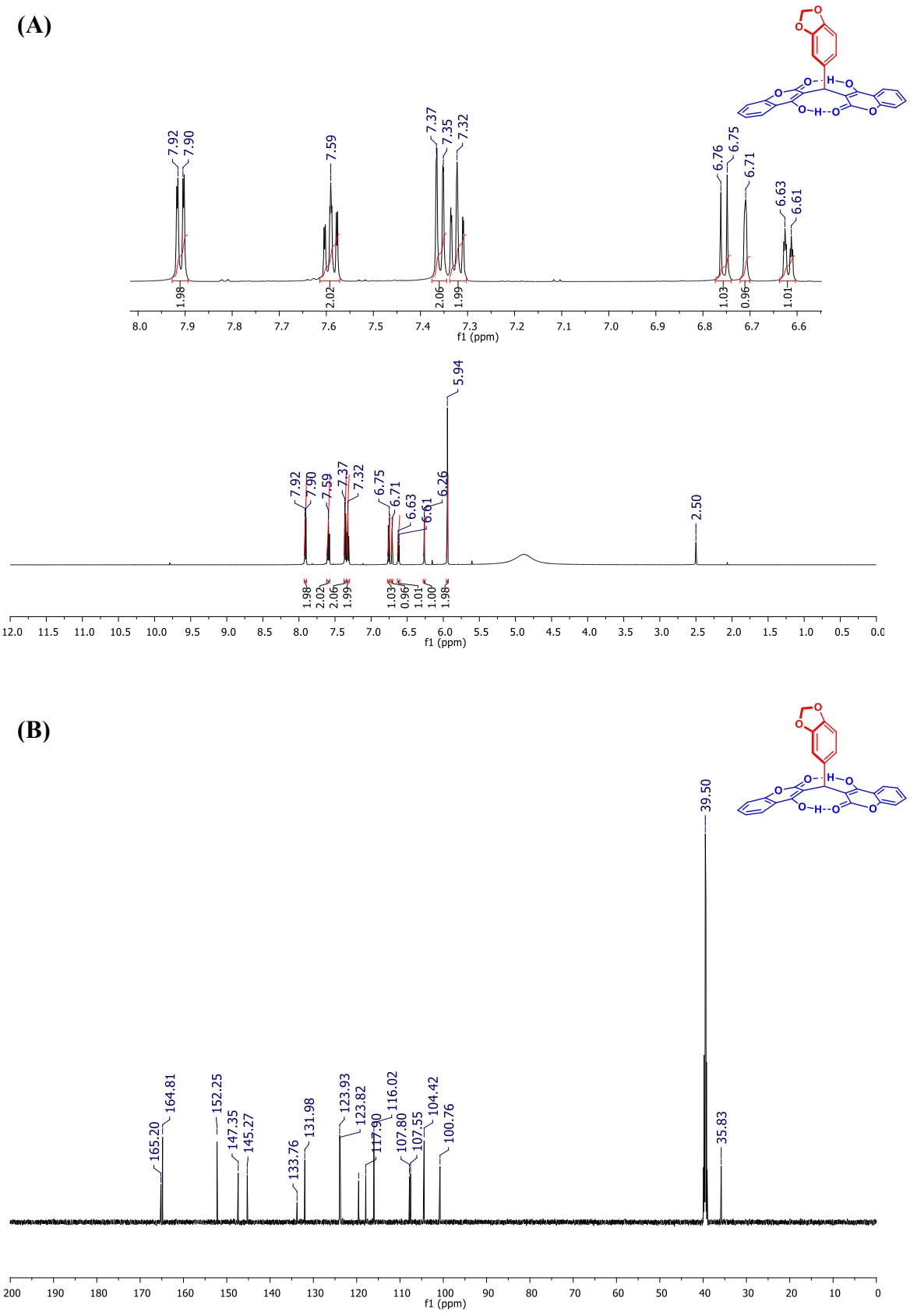

Figure S15. (A) ^{1}H NMR spectrum (600 MHz, DMSO-d_6) of **DC-03.** (B)^{13}C{^{1}H} NMR spectrum (150 MHz, DMSO-d_6) of **DC-03**.

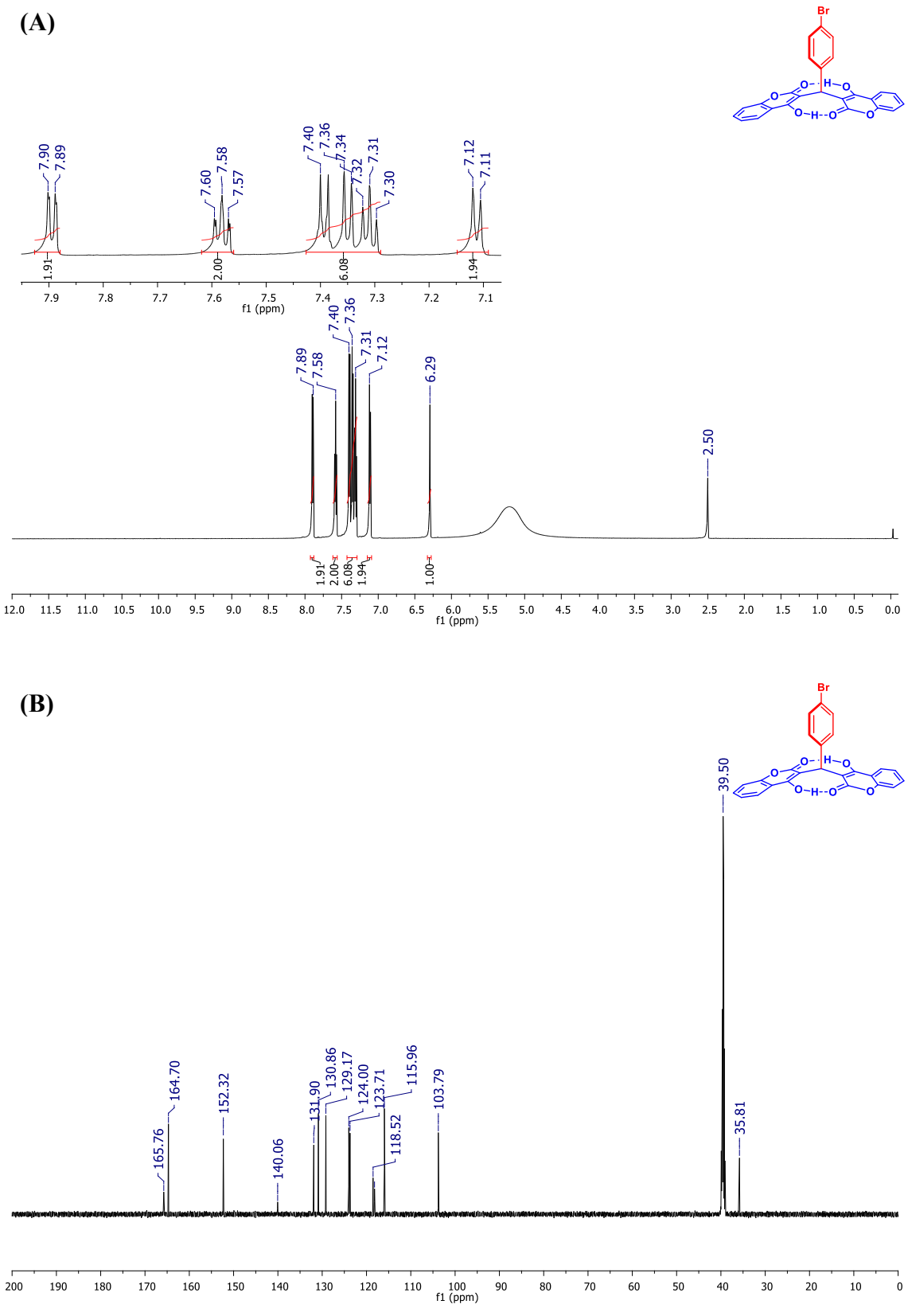

Figure S16. (A) ^{1}H NMR spectrum (600 MHz, DMSO-d_6) of **DC-04.** (B)^{13}C{^{1}H} NMR spectrum (150 MHz, DMSO-d_6) of **DC-04**.

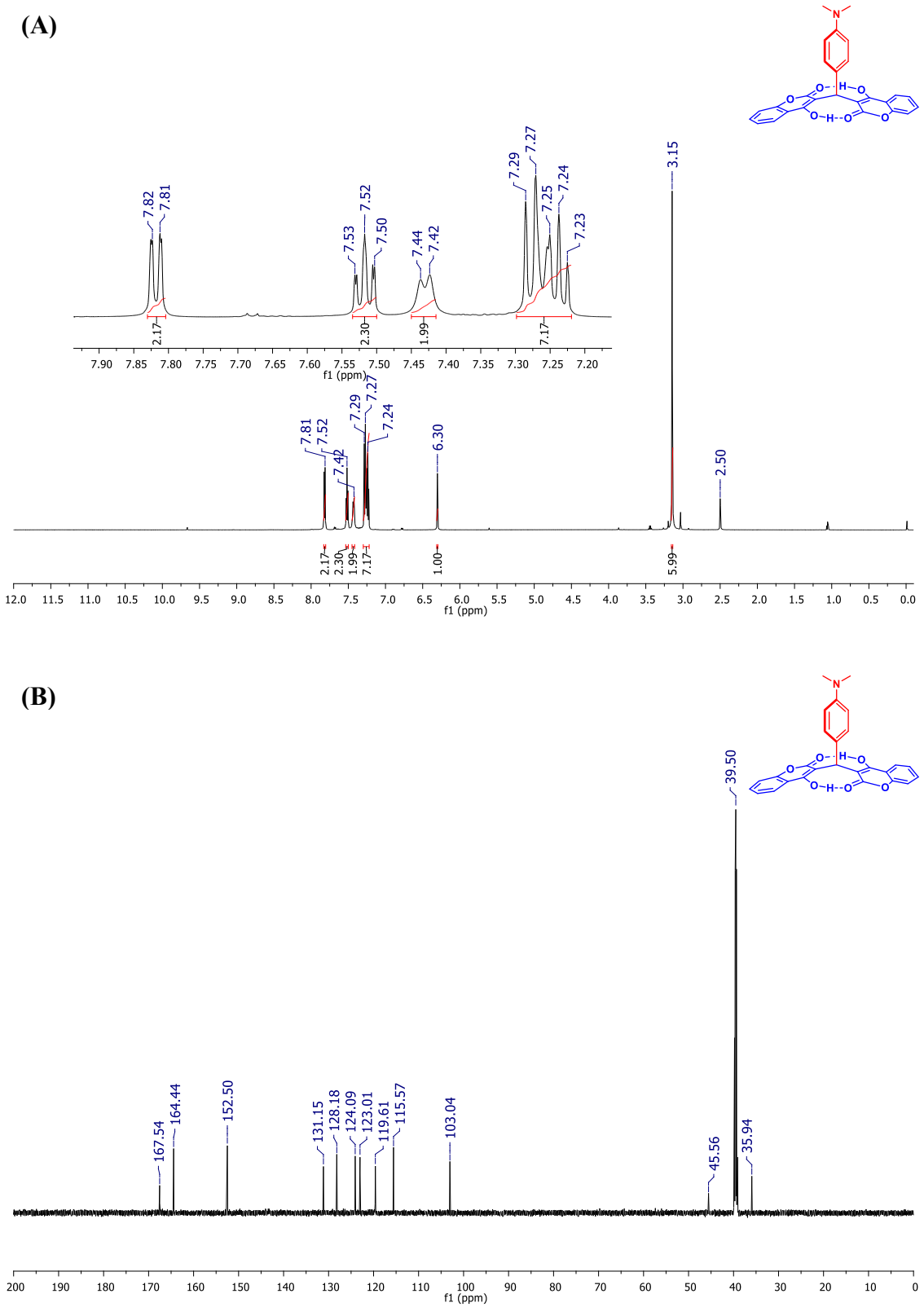

Figure S17. (A) ^{1}H NMR spectrum (600 MHz, DMSO-d_6) of **DC-05.** (B)^{13}C{^{1}H} NMR spectrum (150 MHz, DMSO-d_6) of **DC-05**.

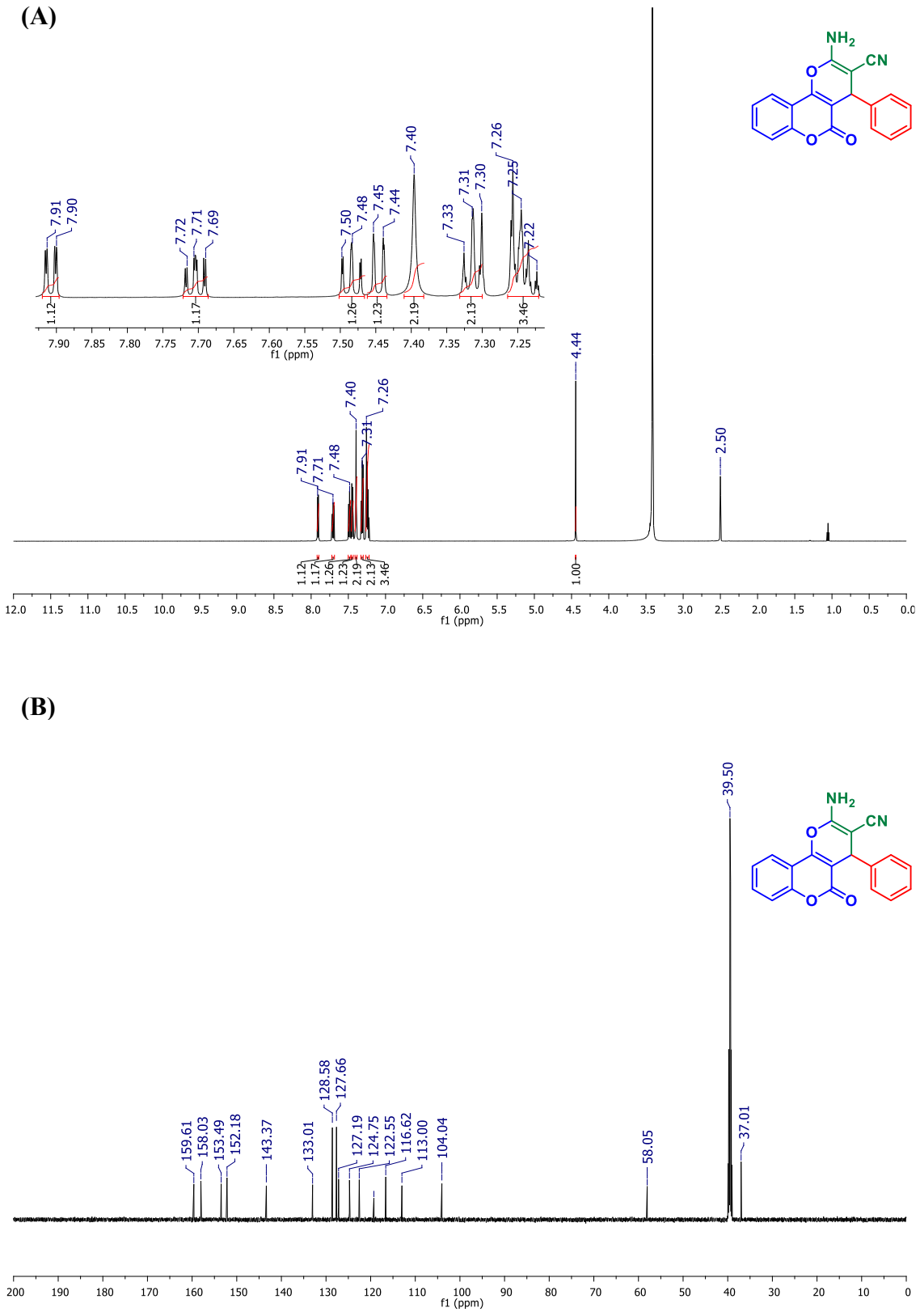

Figure S18. (A) ^{1}H NMR spectrum (600 MHz, DMSO-d_6) of **APC-01.** (B)^{13}C{^{1}H} NMR spectrum (150 MHz, DMSO-d_6) of **APC-01**.

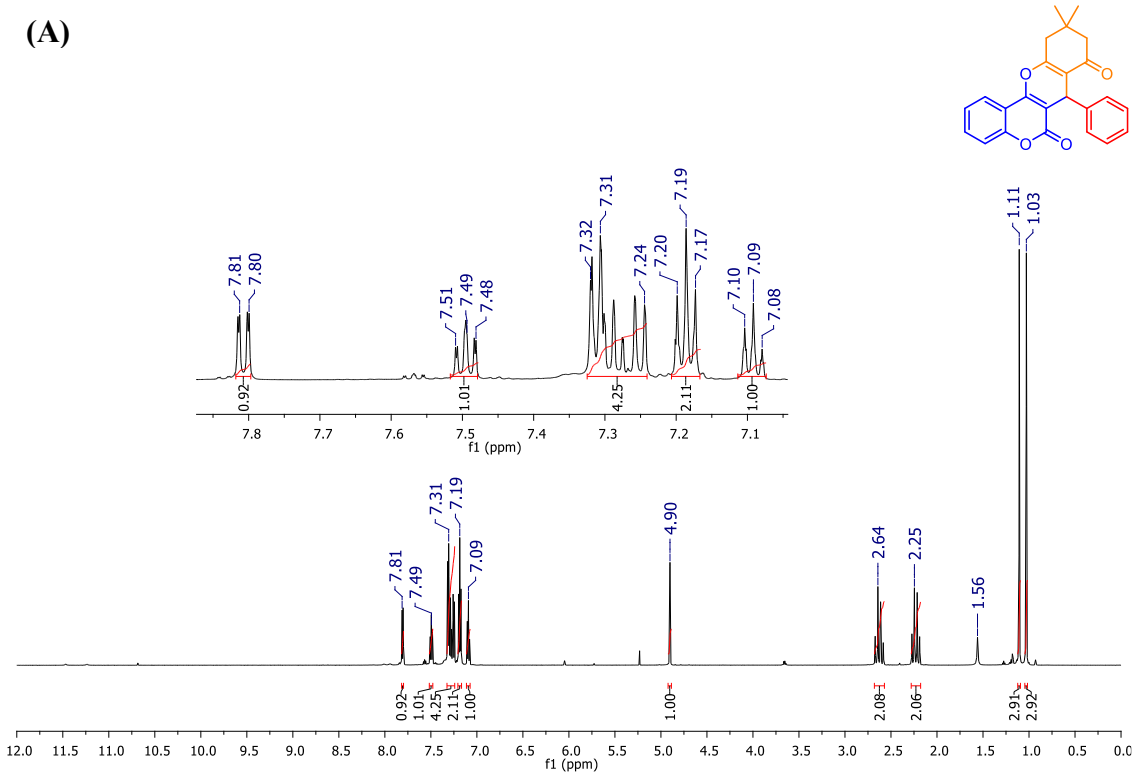

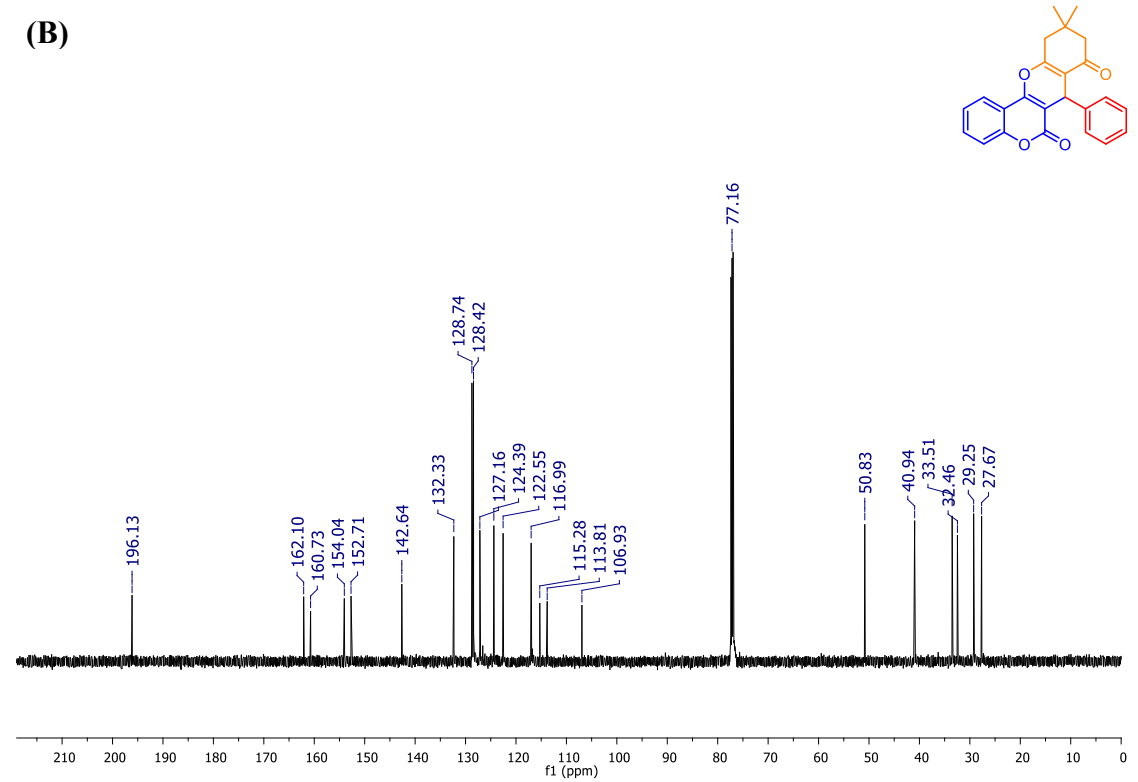

Figure S19. (A) ^{1}H NMR spectrum (600 MHz, $CDCl_3$) of **TCC-01.** (B)$^{13}C\{^{1}H\}$ NMR spectrum (150 MHz, $CDCl_3$) of **TCC-01**.

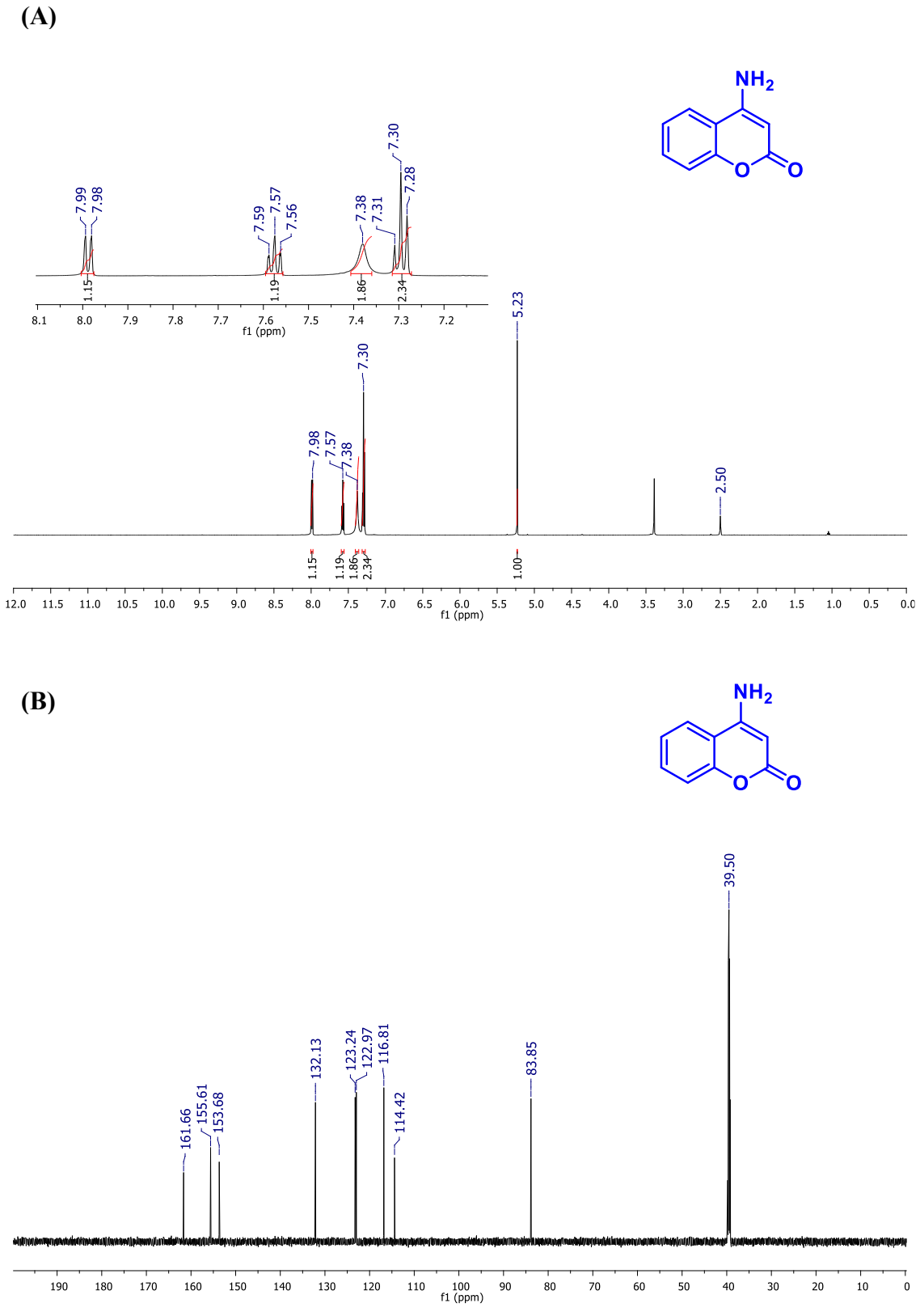

Figure S20. (A) ^{1}H NMR spectrum (600 MHz, DMSO-d_6) of 4-aminocoumarin. (B)^{13}C{^{1}H} NMR spectrum (150 MHz, DMSO-d_6) of 4-aminocoumarin.

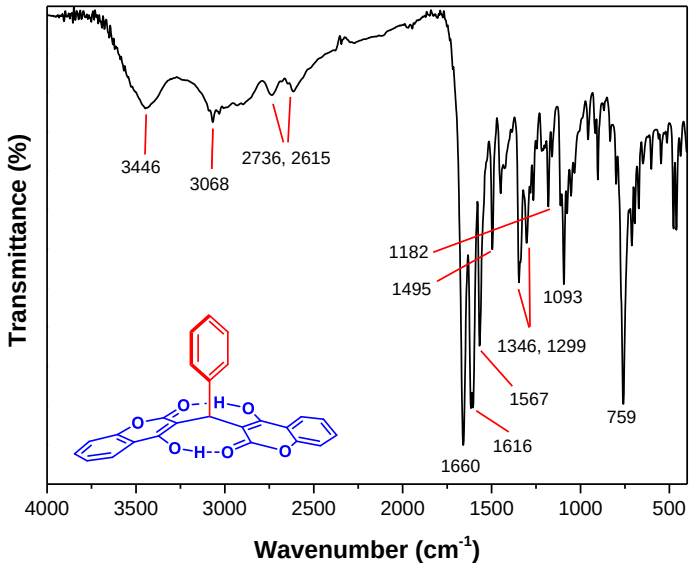

Figure S21. FTIR (KBr) spectrum for **DC-01**.

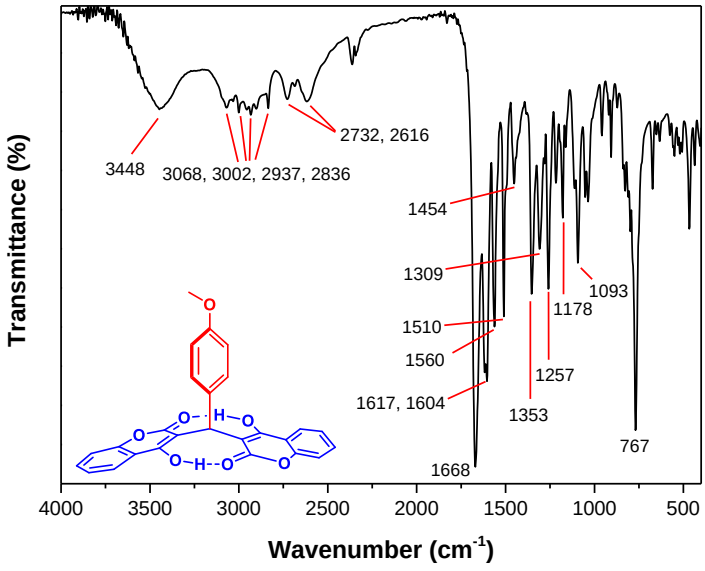

Figure S22. FTIR (KBr) spectrum for **DC-02**.

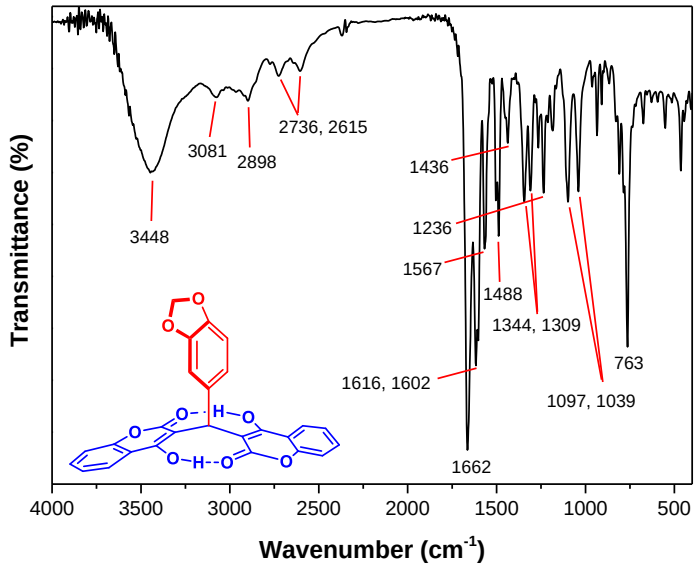

Figure S23. FTIR (KBr) spectrum for **DC-03**.

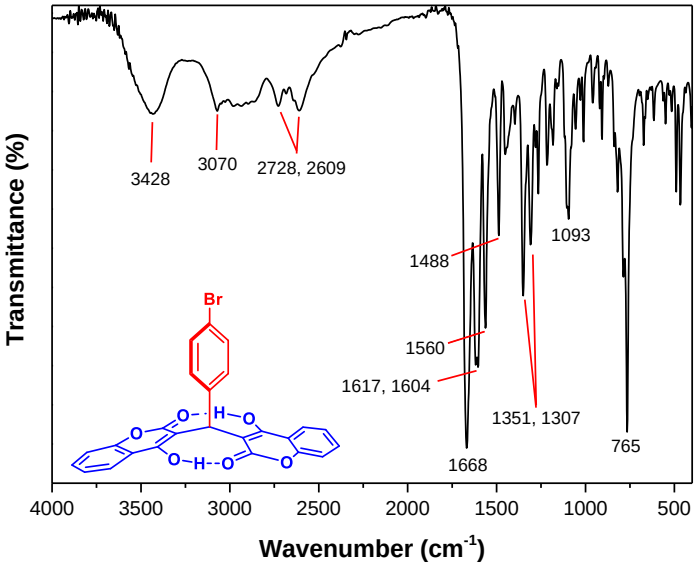

Figure S24. FTIR (KBr) spectrum for **DC-04**.

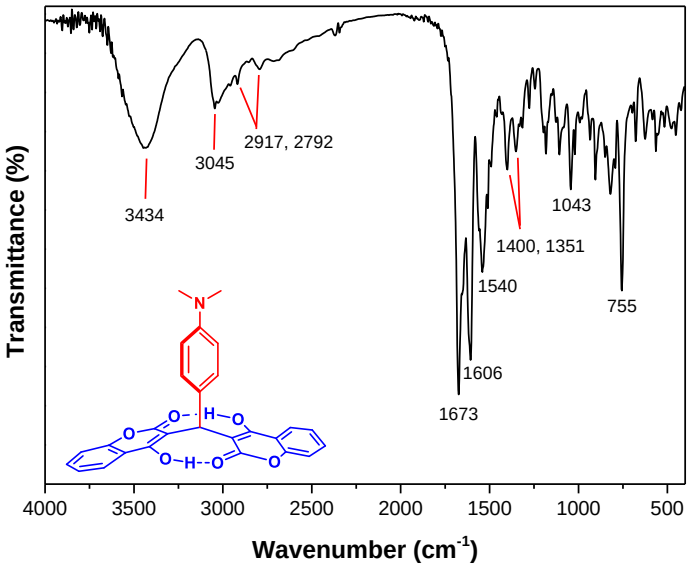

Figure S25. FTIR (KBr) spectrum for **DC-05**.

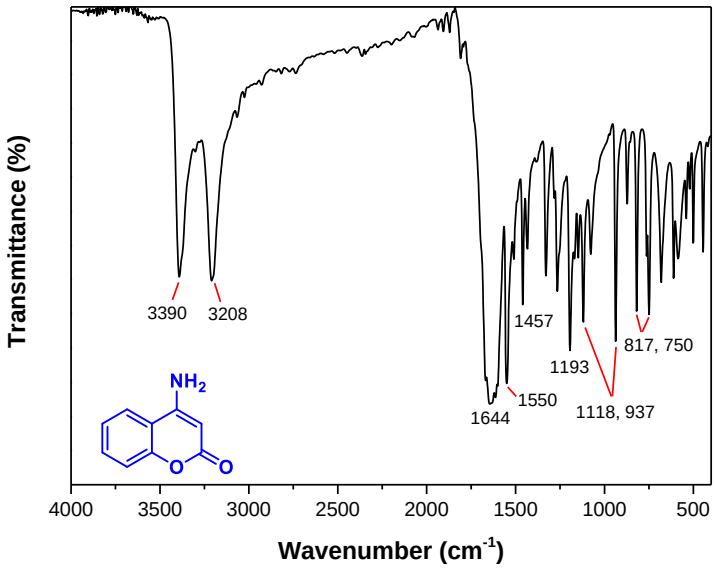

Figure S26. FTIR (KBr) spectrum for 4-aminocoumarin.

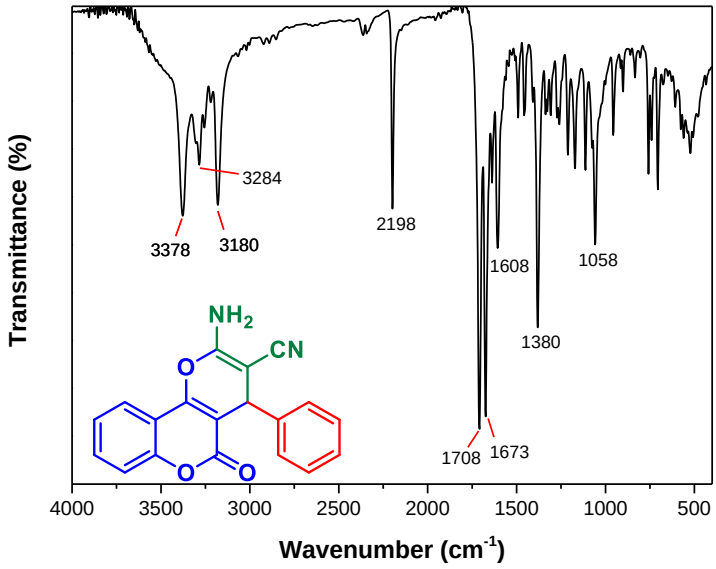

Figure S27. FTIR (KBr) spectrum for **APC-01**.

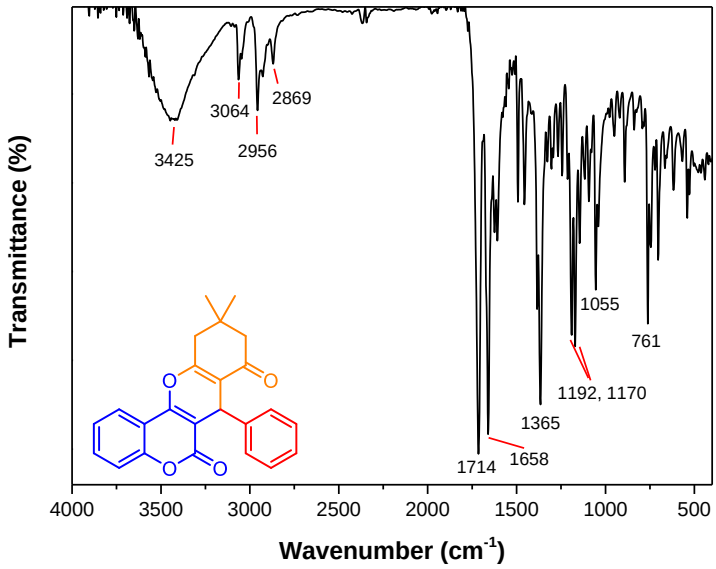

Figure S28. FTIR (KBr) spectrum for **TCC-01**.

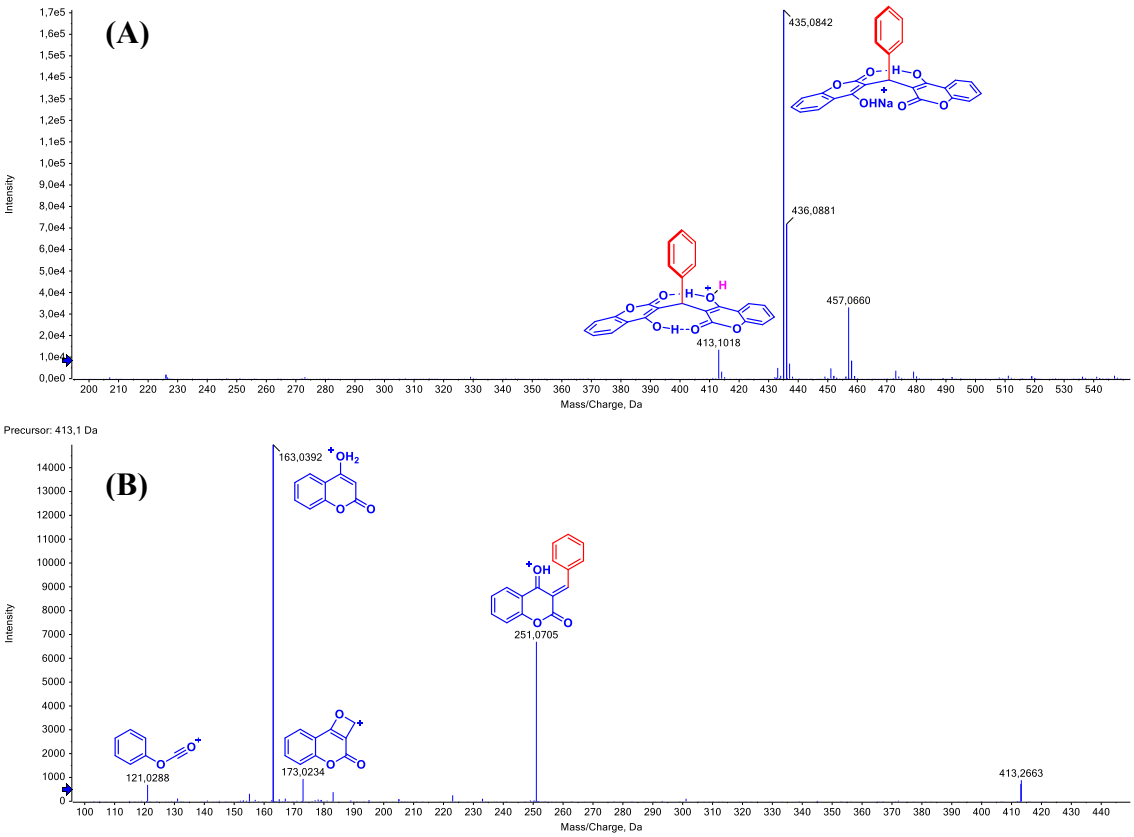

Figure S29. (A) ESI(+)-MS for **DC-01**. (B) ESI(+)-MS/MS for **DC-01**.

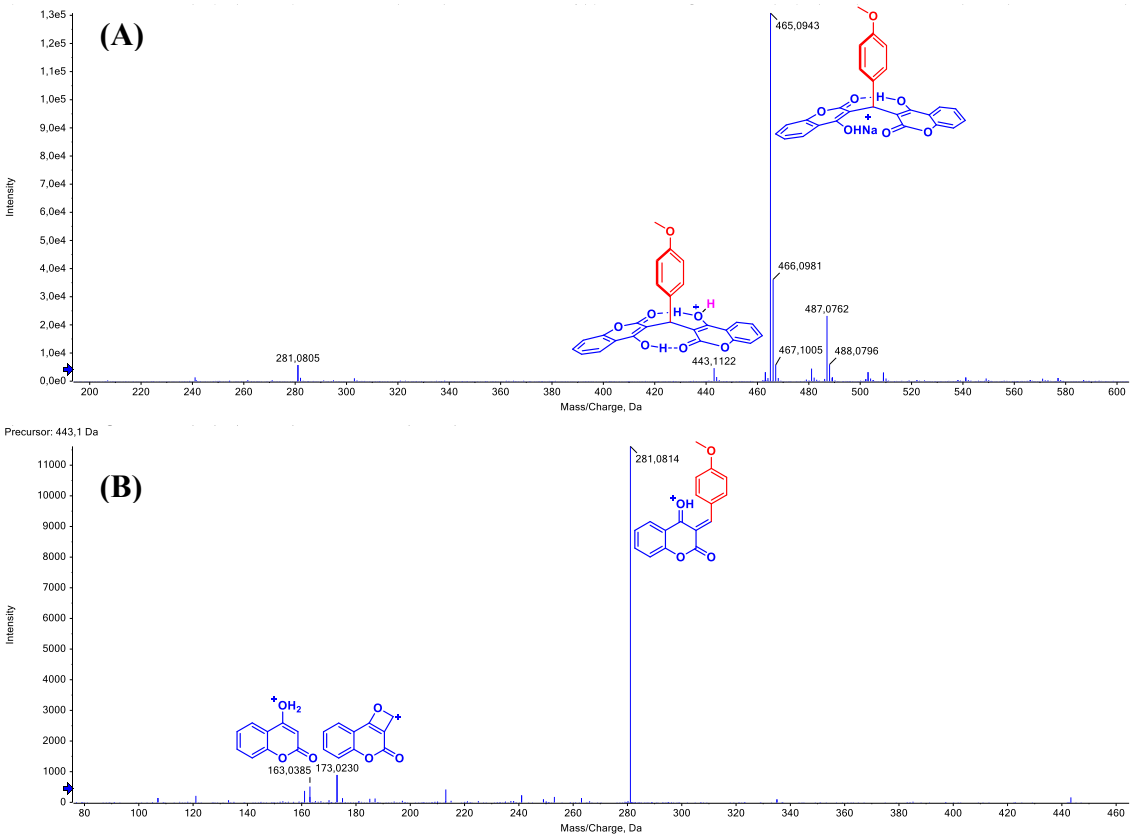

Figure S30. (A) ESI(+)-MS for **DC-02**. (B) ESI(+)-MS/MS for **DC-02**.

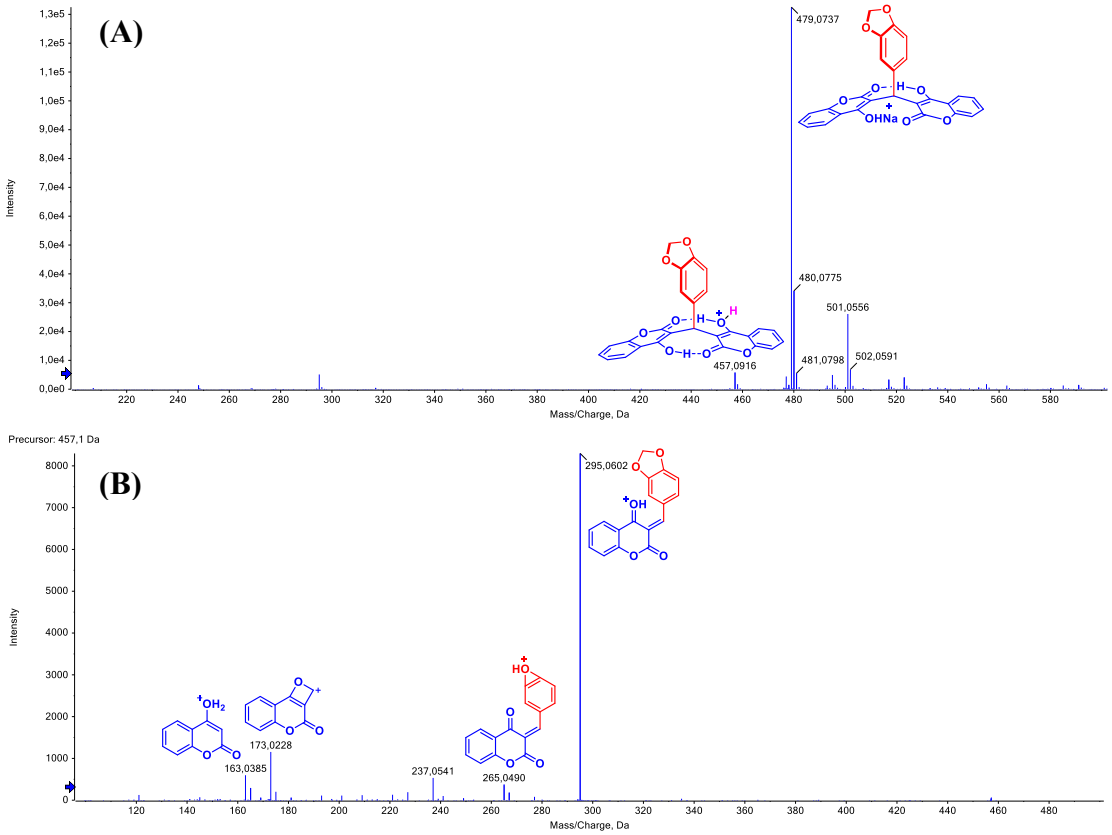

Figure S31. (A) ESI(+)-MS for **DC-03**. (B) ESI(+)-MS/MS for **DC-03**.

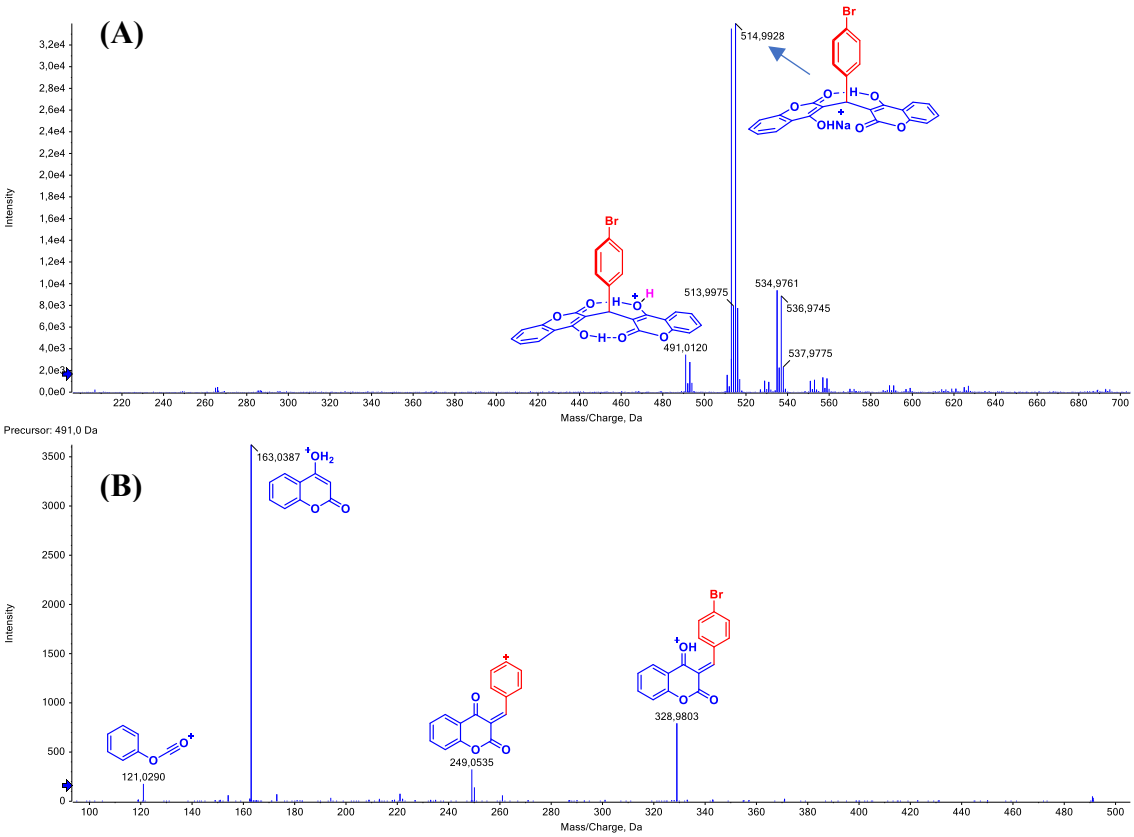

Figure S32. (A) ESI(+)-MS for **DC-04**. (B) ESI(+)-MS/MS for **DC-04**.

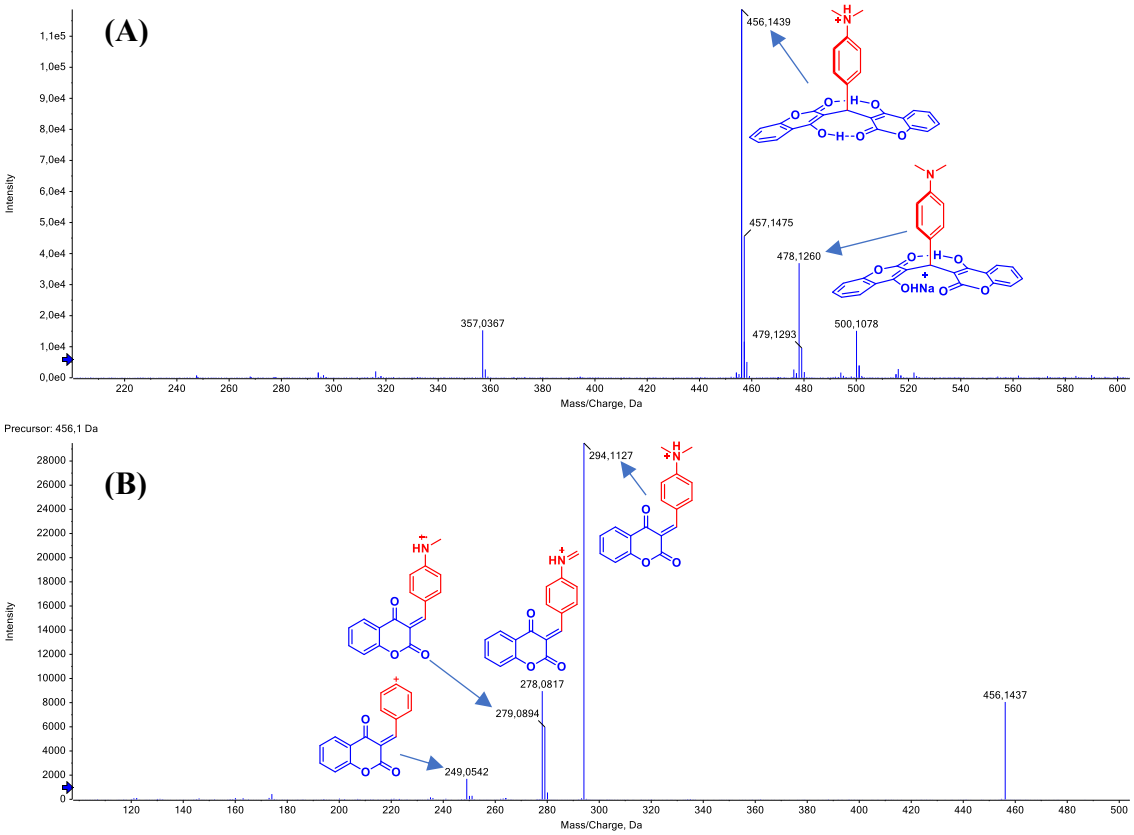

Figure S33. (A) ESI(+)-MS for **DC-05**. (B) ESI(+)-MS/MS for **DC-05**.

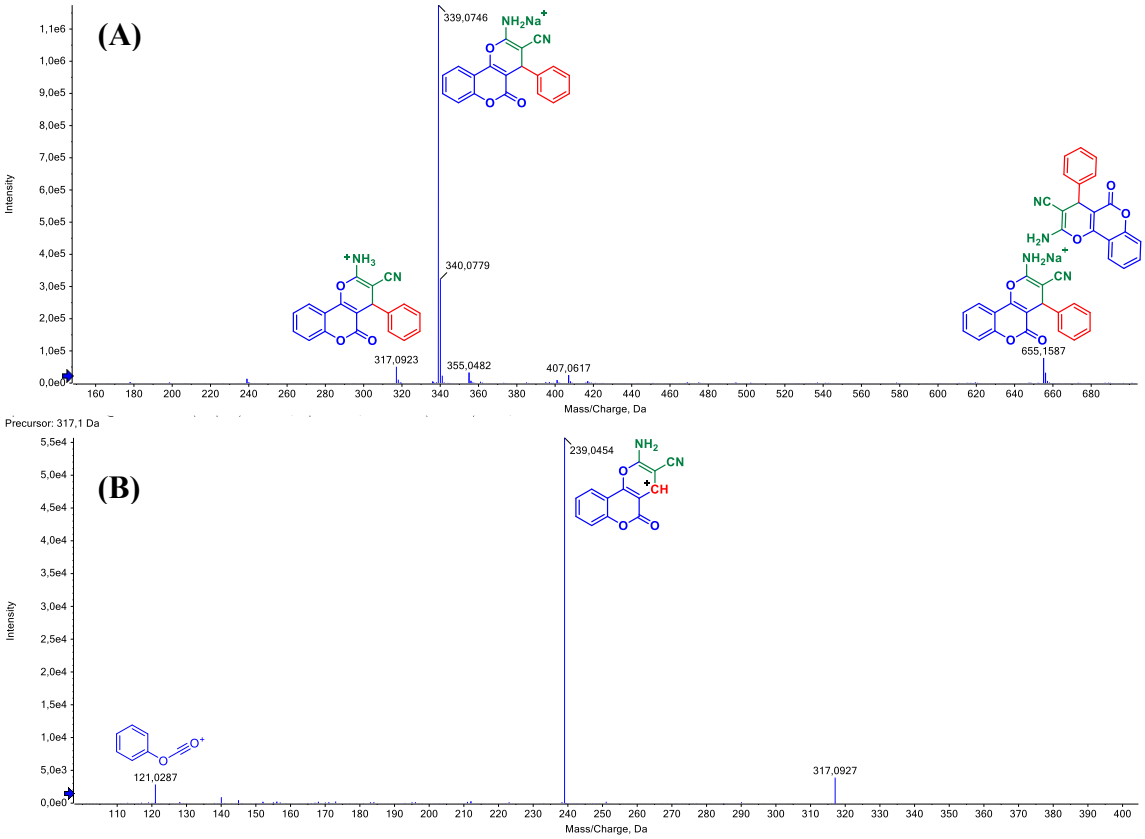

Figure S34. (A) ESI(+)-MS for **APC-01**. (B) ESI(+)-MS/MS for **APC-01**.

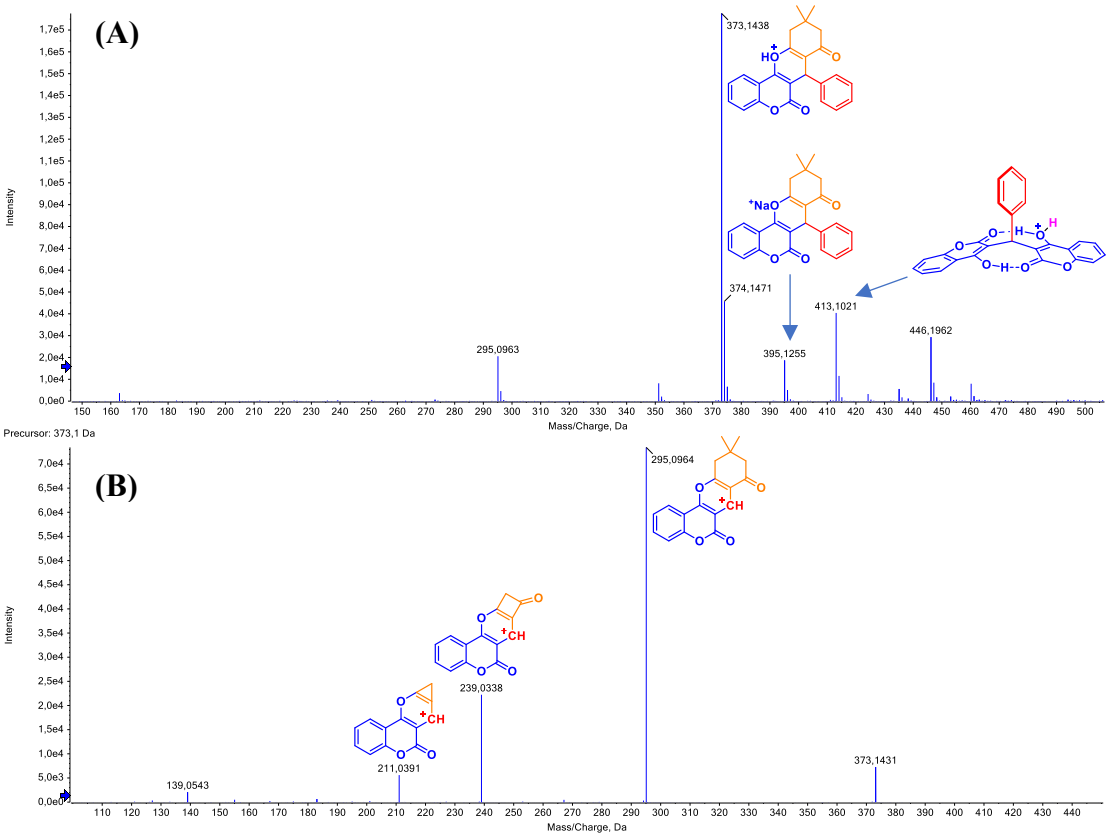

Figure S35. (A) ESI(+)-MS for **TCC-01**. (B) ESI(+)-MS/MS for **TCC-01**.

Determination of numerical values

Productivity is formally expressed as the molar ratio of the produced output to the unreacted limiting reagent. This can be determined through the following equation:

$$Productivity = \frac{n_{product}}{(1 - Yield) * n_{LimitingReactant}} \equiv \frac{Yield}{1 - Yield}$$

Example: In the synthesis of DC-01, 0.297 g of the compound was obtained from a reaction involving 2 mmol of 4-hydroxycoumarin and 1 mmol of benzaldehyde. This yield corresponds to approximately 0.72 mmol, resulting in a 72% yield. Calculating the productivity using the productivity equation, the value for this synthesis is 2.57, as demonstrated below.

$$\frac{0.72\ mmol}{(1 - 0.72) * 1\ mmol} \equiv \frac{0.72}{1 - 0.72} = 2.57$$

The impact of the solvent was investigated by correlating the Kamlet-Taft solvatochromic parameters of each solvent with the natural logarithm of productivity.

References

1. G. Sabitha, G. K. K. Reddy, K. B. Reddy and J. Yadav, *Tetrahedron Lett.*, 2003, **44**, 6497-6499.
2. M. Kidwai, S. Saxena and R. Mohan, *Russ. J. Org. Chem.*, 2006, **42**, 52-55.
3. M. Kidwai, Priya and S. Rastogi, *Z. Naturforsch. B*, 2008, **63**, 71-76.
4. P. K. Ambre, R. R. S. Pissurlenkar, R. D. Wavhale, M. S. Shaikh, V. M. Khedkar, B. Wan, S. G. Franzblau and E. C. Coutinho, *Med. Chem. Res.*, 2014, **23**, 2564-2575.
5. H. Mehrabi and M. Baniasad-Dashtabi, *J. Chem. Res.*, 2015, **39**, 294-295.
6. S. Abdolmohammadi and S. Karimpour, *Chin. Chem. Lett.*, 2016, **27**, 114-118.
7. P. K. Sahu, *RSC Adv.*, 2016, **6**, 67651-67661.
8. S. Sadjadi, M. M. Heravi and M. Malmir, *Res. Chem. Interm.*, 2017, **43**, 6701-6717.
9. S. Sadjadi, M. M. Heravi and M. Malmir, *Appl. Organomet. Chem.*, 2018, **32**, e4286.
10. P. K. Sahu, P. K. Sahu, M. S. Kaurav, M. Messali, S. M. Almutairi, P. L. Sahu and D. D. Agarwal, *ACS Omega*, 2018, **3**, 15035-15042.
11. S. Sadjadi, M. M. Heravi, V. Zadsirjan, S. Y. S. Beheshtiha and R. R. Kelishadi, *ChemistrySelect*, 2018, **3**, 12031-12038.
12. P. K. Sahu, P. K. Sahu, M. S. Kaurav, M. Messali, S. M. Almutairi, P. L. Sahu and D. D. Agarwal, *RSC Adv.*, 2018, **8**, 33952-33959.
13. M. R. Bhosle, D. B. Wahul, G. M. Bondle, A. Sarkate and S. V. Tiwari, *Synth. Commun.*, 2018, **48**, 2046-2060.
14. L. Rout, A. Kumar, P. K. Chand, L. S. K. Achary and P. Dash, *ChemistrySelect*, 2019, **4**, 5696-5706.
15. M. S. Kaurav, P. K. Sahu, P. K. Sahu, M. Messali, S. M. Almutairi, P. L. Sahu and D. D. Agarwal, *RSC Adv.*, 2019, **9**, 3755-3763.
16. J. Puvithra and D. Parthiban, *Asian J. Chem.*, 2020, **32**, 2067-2074.
17. M. M. Heravi, T. Hosseinnejad, M. Tamimi, V. Zadsirjan and M. Mirzaei, *J. Mol. Struct.*, 2020, **1205**, 127598.
18. Y. I. Shaikh, S. S. Shaikh, K. Ahmed, G. M. Nazeruddin and V. S. Shaikh, *Orient. J. Chem.*, 2020, **36**, 415-418.
19. A. K. Bhagi, K. P. Singh, A. Kumar, Priya and N. Manav, *Indian J. Chem.*, 2022, **61**, 1173-1179.
20. Z. Besharati, M. Malmir and M. M. Heravi, *Inorg. Chem. Commun.*, 2022, **143**, 109813.
21. F. Ghobakhloo, D. Azarifar and M. Mohammadi, *J. Phys. Chem. Solids*, 2023, **175**, 111222.
22. P. Ghamari Kargar and G. Bagherzade, *Sci. Rep.*, 2023, **13**, 19104.